

ในกรณีของ stratified smooth flow เราอาจจะสามารถหาค่าของ friction factor โดยใช้ค่า friction factor ของท่อเรียบแทนได้ กรณี wavy interface ก็จะสามารถหาได้ด้วยวิธีเดียวกัน สำหรับกรณีการไหลในแนวดิ่งและแนวเอียงนั้น Wallis et.al.[1] ได้แนะนำค่าที่แสดงความสัมพันธ์ของ interfacial friction factor ในเทอมของความหนาของฟิล์มเฉลี่ย (average film thickness) หรือ Void fraction ไว้ดังนี้

$$f_i = a + b(1 - \alpha)^n \quad (8)$$

โดยที่

a คือ interfacial friction factor ของการไหลในท่อที่ไม่มีของเหลว

$b(1 - \alpha)^n$ คือ ส่วนเสริมที่ได้มาจาก film waviness และ Momentum exchange ซึ่งทำให้เกิด interfacial shear

สำหรับกรณีที่เส้นผ่านศูนย์กลางภายในท่อเท่ากับ 0.051 เมตร Wallis et.al.[1] ได้แนะนำให้ใช้ค่า $a = 0.005$, $b = 24$ และ $n = 2.04$

กรณีการไหลสวนกันในท่อเอียงนั้นค่า interfacial friction factor ไม่สามารถหาได้ด้วยวิธีข้างต้น Cohen and Hanratty [14] ได้แนะนำให้ใช้ $f_i = 0.0142$ Gazley [15] แนะนำสำหรับการไหลตามกันแบบราบเรียบ ในกรณีที่ความเร็วของก๊าซมีค่ามากกว่าความเร็วของของไหลมากๆ ค่าของ f_i จะเท่ากับ f_g

การวิเคราะห์การเกิด CCFL ในท่อซึ่งวางอยู่ในแนวเอียงจะเริ่มพิจารณาจากการไหลสวนกันแบบแยกชั้น โดยที่ของเหลวจะไหลเป็นแผ่นบางผ่านลงไปตามผนังของท่อและก๊าซไหลสวนทางขึ้นไป ที่ผิวสัมผัสของของไหลจะมีคลื่นเกิดอยู่ที่ผิวของเหลวเนื่องจากพื้นที่หน้าตัดลดลง ก๊าซจะมีอัตราเร่งเพิ่มขึ้น ซึ่งเป็นสาเหตุให้คลื่นมีขนาดโตขึ้นส่งผลให้เกิดความไม่สมดุลยขึ้นที่ผิวสัมผัสของของไหลทั้งสองจนกระทั่งสามารถเอาชนะแรงเนื่องจากแรงโน้มถ่วง รูปแบบของการไหลจะเปลี่ยนไปจากการไหลสวนกันเป็นการไหลตามกัน Taitel and Dukler[16] แนะนำให้ใช้ข้อจำกัดสำหรับกรณี unstable interface ซึ่งคลื่นจะยังคงมีขนาดใหญ่ขึ้นและของเหลวจะถูกกวาดไปในทิศทางของการไหลของก๊าซในรูปของ slug หรือ waves ไว้ดังนี้

$$U_G = \left(1 - \frac{h_L}{D}\right) \left[\frac{(\rho_L - \rho_G)g \cos \beta A_G}{\rho_G dA_L / dh_L} \right]^{1/2} \quad (9)$$

โดยที่เราสามารถหา dA_L / dh_L ได้จาก

$$dA_L / dh_L = \sqrt{1 - (2h_L - 1)^2} \quad (10)$$

สมการทั้งหมดจะถูกนำมาประกอบกันเป็นแบบจำลองทางคณิตศาสตร์ เพื่อทำนายการจำกัดในการไหลสวนกัน flow chart ของการคำนวณแสดงได้ดังรูปที่ 2

ผลจากแบบจำลอง

สำหรับแบบจำลองทางคณิตศาสตร์ที่สร้างขึ้นโดยใช้ อากาศแทนก๊าซ และน้ำแทนของเหลวที่อุณหภูมิเฉลี่ย 30° ในท่อขนาดเส้นผ่านศูนย์กลาง 0.051 เมตร ที่มุมเอียงของท่อตั้งแต่ 30° - 80° จากแนวนอน แสดงให้เห็นดังรูปที่ 3 ถึง 8 โดยแสดงผลของสภาวะในการเกิด CCFL ในเทอมของความเร็วเทียมของน้ำ (U_{LS}) และความเร็วเทียมของอากาศ (U_{GS}) ซึ่งเป็นเทอมที่นิยมใช้กันในสาขาวิชานี้และสามารถหาได้โดยการนำอัตราไหลของของไหลแต่ละชนิดหารด้วยพื้นที่หน้าตัดของท่อ

เมื่อพิจารณาผลลัพธ์ที่ได้ (รูปที่ 3 ถึง 8) พบว่าแนวโน้มการเกิด CCFL จะเป็นไปในทางเดียวกัน คือที่ความเร็วของอากาศต่ำความเร็วของน้ำที่ CCFL จะสูง และที่ความเร็วของอากาศสูงความเร็วของน้ำที่ CCFL จะต่ำ เมื่อแบ่งการพิจารณาออกเป็นสองช่วงคือ ที่มุมเอียงของท่อปานกลาง 30° - 60° จากแนวนอน (รูปที่ 3 ถึง 6) และที่มุมเอียงของท่อสูง 70° - 80° จากแนวนอน (รูปที่ 7 ถึง 8) พบว่าในช่วงแรกที่ความเร็วของอากาศคงที่ พบว่าความเร็วของน้ำที่ CCFL จะสูงขึ้นเมื่อมุมเอียงของท่อเพิ่มมากขึ้น ในช่วงที่สองที่มุมเอียงของท่อ 70° (รูปที่ 7) ที่ความเร็วของอากาศคงที่ในช่วงต่ำถึงปานกลางความเร็วของน้ำที่ CCFL จะต่ำกว่าที่มุมเอียง 80° (รูปที่ 8) และที่ความเร็วของอากาศคงที่ในช่วงปานกลางถึงสูงความเร็วของน้ำที่ CCFL จะสูงกว่าที่มุมเอียง 80° เมื่อเปรียบเทียบผลระหว่างช่วงแรกและช่วงที่สอง พบว่าที่ความเร็วของอากาศคงที่ในช่วงต่ำถึงปานกลางความเร็วของน้ำที่ CCFL ในช่วงแรกจะต่ำกว่าในช่วงที่สอง และที่ความเร็วของอากาศคงที่ในช่วงปานกลางถึงสูงความเร็วของน้ำที่ CCFL ในช่วงแรกจะสูงกว่าในช่วงที่สอง ผลกระทบของมุมเอียงในช่วงแรกนั้นมุมเอียงที่เปลี่ยนแปลงไป จะมีผลต่อการเกิด CCFL ไม่มากนัก แต่เมื่อท่อมีมุมเอียงใกล้เคียงแนวตั้งมากขึ้น ผลกระทบของมุมเอียงที่เปลี่ยนแปลงจะมีผลต่อการเกิด CCFL มากขึ้น สาเหตุที่เป็นเช่นนี้เนื่องจากมุมเอียงของท่อที่เปลี่ยนแปลงไปจะมีผลต่อค่าพารามิเตอร์ ในสมการที่ (3) และ (10) และเมื่อมุมเอียงของท่อใกล้เคียงแนวตั้งมากรูปแบบของการไหลจะเปลี่ยนจากการไหลแบบแยกชั้นเป็นการไหลแบบวงแหวนทำให้พื้นที่ผิวสัมผัสระหว่างของไหลทั้งสองมากขึ้น อย่างไรก็ตามการเปลี่ยนรูปแบบของการไหลนั้นจะขึ้นกับความเร็วของของไหลทั้งสองด้วย

สรุป

การศึกษาการเกิดCCFL จากแบบจำลองทางวิทยาศาสตร์ที่สร้างขึ้นมาสามารถใช้ทำนายปรากฏการณ์ที่เกิดขึ้นโดยปราศจากการทดลอง ผลจากแบบจำลองทางคณิตศาสตร์พบว่า

1.การเกิดCCFL จะมีแนวโน้มไปในทางเดียวกัน คือในช่วงความเร็วของอากาศต่ำ ความเร็วของน้ำที่CCFL จะสูง และในช่วงความเร็วของอากาศสูงความเร็วของน้ำที่CCFL จะต่ำ

2.ที่มุมเอียงของท่อปานกลาง 30° - 60° จากแนวนอน เมื่อพิจารณาที่ความเร็วของอากาศคงที่ พบว่าความเร็วของน้ำจะสูงขึ้น เมื่อมุมเอียงของท่อเพิ่มมากขึ้น

3.ที่มุมเอียงของท่อสูง 70° - 80° จากแนวนอน เมื่อพิจารณา ที่ความเร็วของอากาศคงที่ พบว่าในช่วงที่ความเร็วของอากาศต่ำท่อที่มีมุมเอียง 70° จะมีความเร็วของที่CCFL ต่ำกว่าท่อที่มีมุมเอียง 80° และในช่วงที่ความเร็วของอากาศสูงท่อที่มีมุมเอียง 70° จะมีความเร็วของน้ำที่CCFL สูงกว่าท่อที่มีมุมเอียง 80°

4.เมื่อเปรียบเทียบผลระหว่างท่อที่มีมุมเอียงปานกลาง และท่อที่มีมุมเอียงสูงเมื่อพิจารณาที่ความเร็วของอากาศคงที่พบว่า ในช่วงที่ความเร็วของอากาศต่ำ ความเร็วของน้ำที่CCFL ของท่อที่มีมุมเอียงปานกลางจะต่ำกว่าท่อที่มีมุมเอียงสูง และในช่วงที่ความเร็วของอากาศสูงความเร็วของน้ำที่CCFL ของท่อที่มีมุมเอียงปานกลาง จะสูงกว่าท่อที่มีมุมเอียงสูง

สาเหตุที่เป็นเช่นนี้ เนื่องจากมุมเอียงของท่อที่เปลี่ยนไป นั้นจะทำให้พื้นที่ผิวสัมผัสระหว่างของไหลทั้งสองเปลี่ยนแปลงตามไปด้วย ดังสมการที่ (3) และสมการที่ (10)

ที่มุมเอียงของท่อปานกลางผลกระทบของมุมเอียงที่เปลี่ยนแปลงไป จะไม่แตกต่างกันมากนัก แต่จะมีผลกระทบมากขึ้นเมื่อมุมเอียงของท่อเข้าใกล้แนวตั้งมากขึ้น และเพื่อให้มั่นใจในการจำลองแบบจำลองทางคณิตศาสตร์ที่พัฒนาขึ้นมาจำเป็นต้องมีผลลัพธ์จากการทดลองมายืนยันผล ซึ่งจะได้นำเสนอในโอกาสต่อไป

รายการสัญลักษณ์

- A = พื้นที่หน้าตัดของท่อ, m^2
 A_L = พื้นที่หน้าตัดของของเหลว, m^2
 A_G = พื้นที่หน้าตัดของก๊าซ, m^2
 a = ค่าคงที่สำหรับสมการที่(8)
 b = ค่าคงที่สำหรับสมการที่(8)
 C = ค่าคงที่ของสัดส่วนแรงเสียดทานระหว่างผิวสัมผัส
 d = เส้นผ่านศูนย์กลางท่อ, m
 D_L = เส้นผ่านศูนย์กลางไฮดรอลิกของของเหลว, m
 D_G = เส้นผ่านศูนย์กลางไฮดรอลิกของก๊าซ, m
 f_L = แฟคเตอร์แรงเสียดทานระหว่างผิวสัมผัสของของเหลวและผิวท่อ
 f_G = แฟคเตอร์แรงเสียดทานระหว่างผิวสัมผัสของของก๊าซและผิวท่อ
 f_i = แฟคเตอร์แรงเสียดทานระหว่างผิวสัมผัสของของเหลวและก๊าซ
 g = ความเร่งเนื่องจากแรงโน้มถ่วงของโลก, $m/วินาที^2$
 h_L = ระดับของของเหลวภายในท่อ, m
 m = ค่าคงที่ในสมการของแรงเสียดทานระหว่างผิวสัมผัส
 n = ค่าคงที่ในสมการของแรงเสียดทานระหว่างผิวสัมผัส
 P = ความดัน, นิวตัน/ m^2
 S_L = , Perimeter ระหว่างของเหลวและผิวท่อ, m
 S_G = Perimeter ระหว่างของก๊าซและผิวท่อ, m
 S_i = Perimeter ระหว่างของเหลวและก๊าซ, m
 U_L = ความเร็วเฉลี่ยของของเหลว, $m/วินาที$
 U_G = ความเร็วเฉลี่ยของก๊าซ, $m/วินาที$
 U_{Ls} = ความเร็วเทียมของของเหลว, $m/วินาที$
 U_{Gs} = ความเร็วเทียมของก๊าซ, $m/วินาที$
 α = ค่าคงที่ในสมการที่(8)
 β = มุมเอียงของส่วนทดสอบ, องศา
 V_L = ความหนืดจลน์ศาสตร์ของของเหลว, $m^2/วินาที$
 V_G = ความหนืดจลน์ศาสตร์ของก๊าซ, $m^2/วินาที$

ρ_L = ความหนาแน่นของของเหลว, ก.ก./ม³

ρ_G = ความหนาแน่นของก๊าซ, ก.ก./ม²

τ_L = แรงเฉือนระหว่างของเหลวและผิวท่อ, นิวตัน/ม²

τ_G = แรงเฉือนระหว่างก๊าซและผิวท่อ, นิวตัน/ม²

τ = แรงเฉือนระหว่างของเหลวและก๊าซ, นิวตัน/ม²

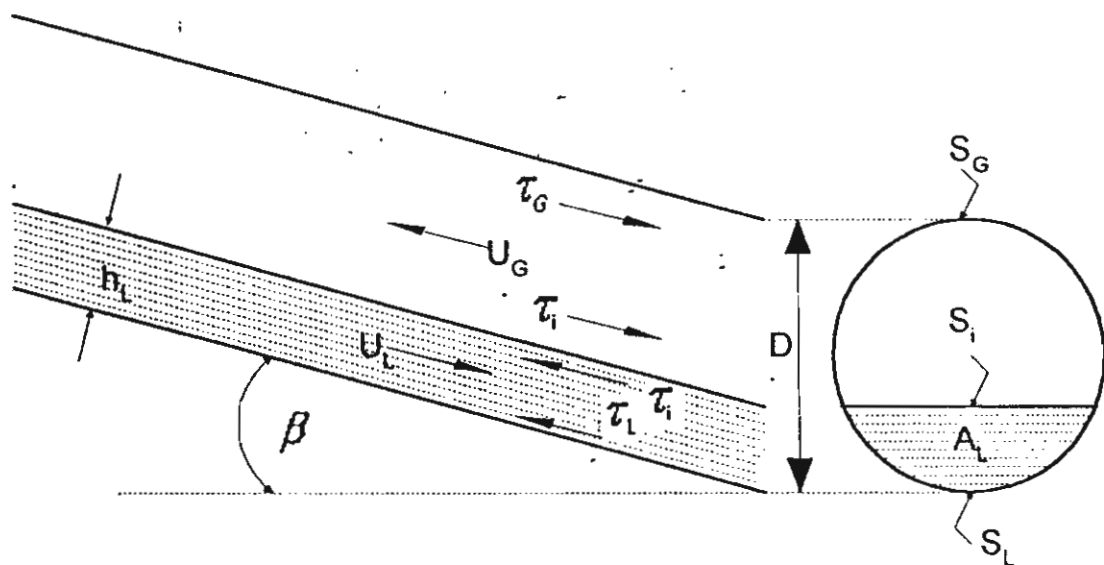
กิตติกรรมประกาศ

ผู้เขียนขอขอบพระคุณสำนักงานกองทุนสนับสนุนการวิจัย (สกว) ที่ได้สนับสนุนด้านการเงินในการดำเนินงาน (ทุนวิจัยเลขที่ RSA 3880019)

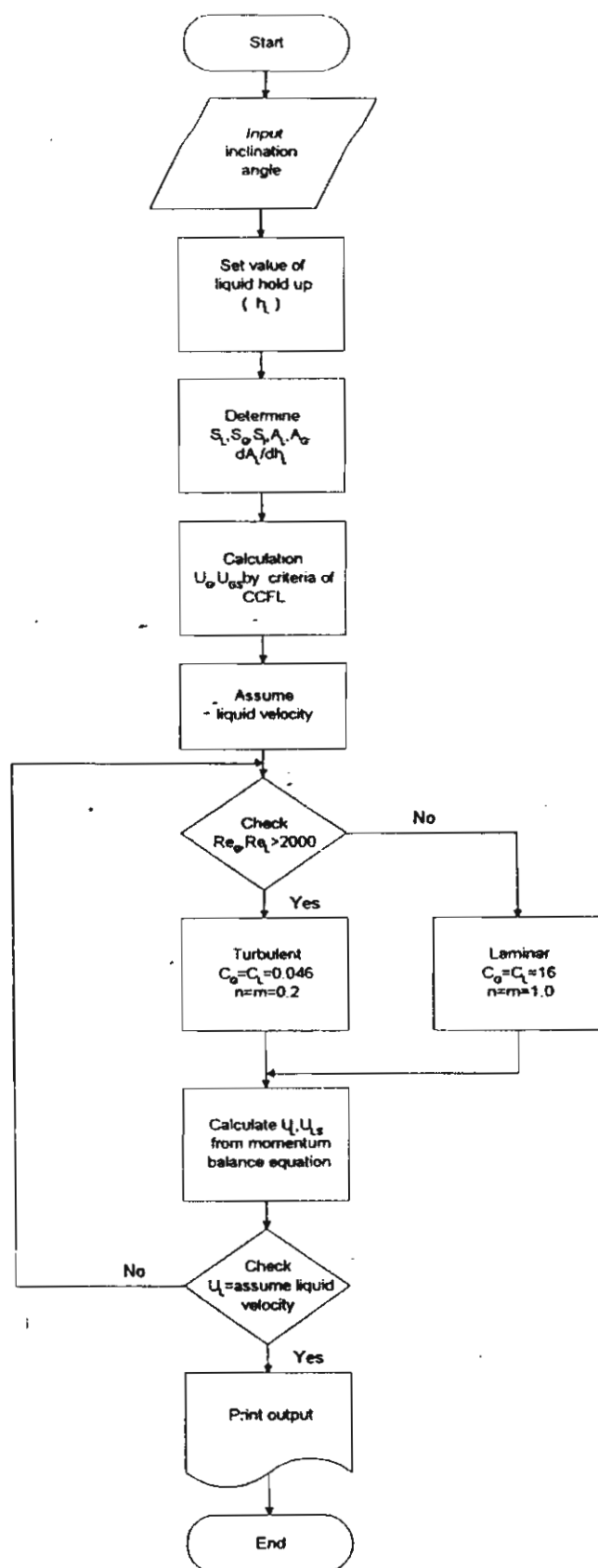
เอกสารอ้างอิง

1. Wallis, G.B., Richter, H.J. and Bharathan, D., 1979, "Air-Water Countercurrent Annular Flow, " Electric Power Research Institute Rep., EPRI NP-1165.
2. Tien, C.L., Chung, K.S., and Liu, C.P., 1980, "Flooding in Two Phase Countercurrent Flows, " Physico Chemical Hydrodynamics, No. 1, pp. 195-220.
3. Hewitt, G.F., 1977, "Influence of End Condition, Tube Inclination and Fluid Physical Properties on Flooding Gas-Liquid Flows, " Harwall Report, HTFS-RS222.
4. Lee, S.C. and Bankoff, S.G., 1983, "Stability of Steam-Water Countercurrent Flow in an Inclined Channel: Flooding, " J. Heat Transfer, No.105, pp. 713-718.
5. Barner, D., Shoham, O. and Taitel, Y., 1982, "Flow Pattern Transition for Downward Inclined Two Phase Flow: Horizontal to Vertical, " Chemical Engineering Science, No. 37, pp. 735-740.
6. Beckmann, H and Mewes, D , 1991, "Experimental Studies of Countercurrent Flow in Inclined Tubes, " European Two Phase Flow Group Meeting.
7. Gardner, G.C., 1983, "Flooded Countercurrent Two-Phase Flow in Horizontal Tubes and Channel, " Int.J.Multiphase Flow, Vol.9, No.4, pp. 367-382.
8. Hewitt, G.F., Lacey, P.M.C. and Nicholis, B., 1965, "Transition in Film Flow in a Vertical Tube, " AERE-R 4614.
9. Daly, B.J. and Harlow, F.H., 1981, "A Model of Countercurrent Steam-Water Flow in Large Horizontal Pipes, " Nuclear Science and Engineering, No.77, pp. 273-284.
10. Shearer, C.J. and Davidson, J.F., 1965, "The Investigation of Standing Wave Due to Gas Blowing Upward Over a Liquid Film; Its Relation to Flooding in Watted Wall Columns, " J. Fluid Mechanic, No. 22, pp. 321-335.
11. Centinbudakler, A.G. and Jameson, G.J., 1969, "The Mechanism of Flooding in Vertical Countercurrent Two Phase Flow, " Chemical Engineering Science, No.24, pp. 1669-1680.
12. Imura, H., Kusuda, H. and Fanotsu, S., 1977. "Flooding Velocity in a Countercurrent Annular Two-Phase Flow, " Chemical Engineering Science, No.32, pp. 49-87.

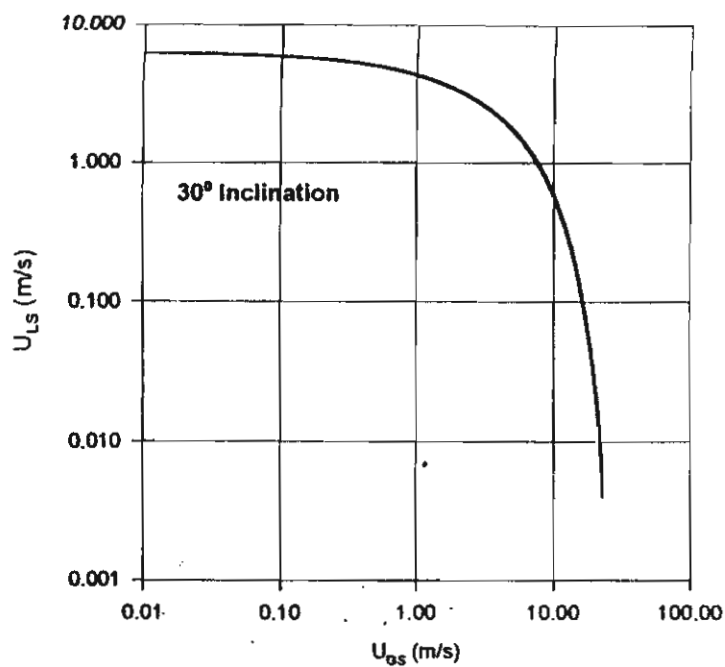
13. Agrawal, S.S., Gregory, G.A., and Govier, G.W., 1973 "An analysis of horizontal stratified two-phase flow in pipes, " Can. J. Chem. Eng, No.51, pp. 280-286.
14. Gazley, C., 1964. "Interfacial Shear and Stability in Two-Phase Flow, "PhD thesis, University of Delaware., New York.
15. Choen, S.L. and Hanratty, T.J., 1968, "Effect of Waves at a Gas-Liquid Interface on a Turbulent Airflow, " Fluid Mechanics, No.31, pp. 467-469.
16. Taitel, Y. and Dukler, A.E., 1976, "A Model for Predicting Flow Regime Transition in Horizontal and Near Horizontal Gas-Liquid Flow, " AIChE, pp. 47-55.
17. Wallis, G.B., Richter, H.J. and Bharathan, D., 1978, "Air-Water Countercurrent Annular Flow in Vertical Tubes, " Electric Power Research Institute Rep., EPRI NP-786.



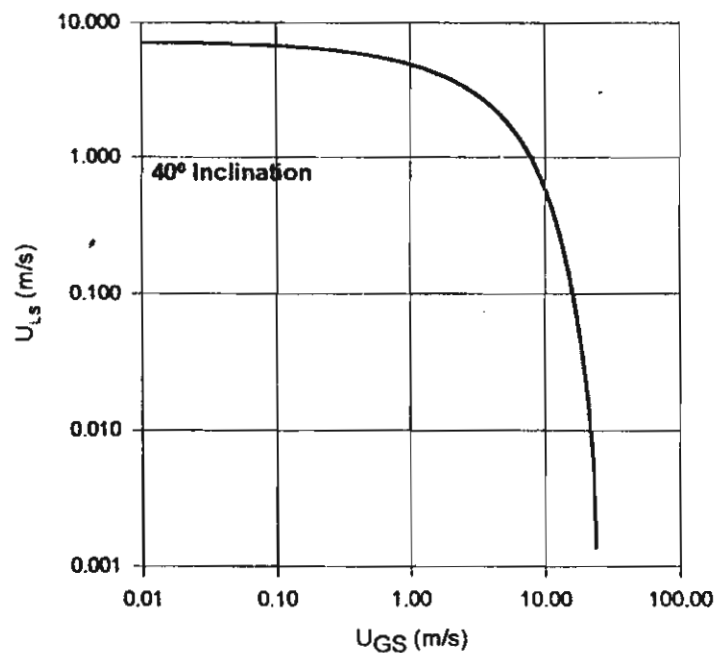
รูปที่ 1 การไหลสวนกันของของไหลสองสถานะแบบแยกชั้น



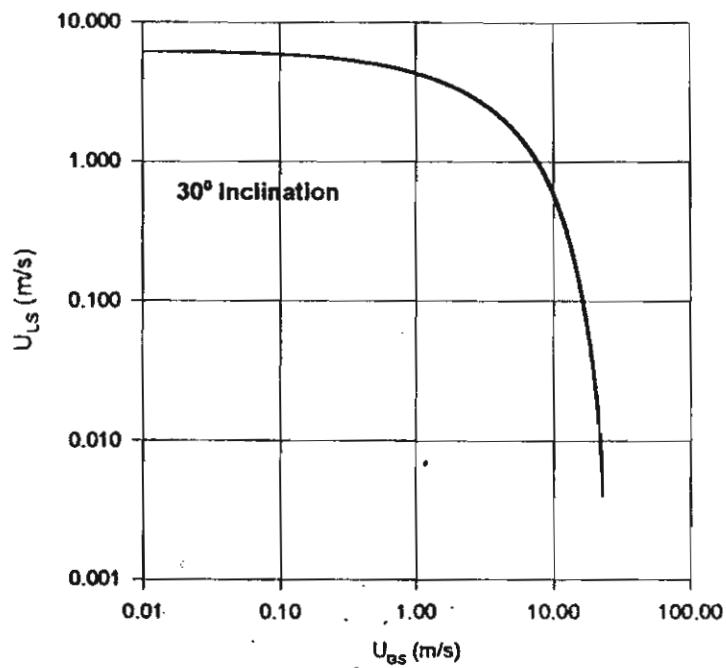
รูปที่ 2 แผนภูมิโปรแกรมคอมพิวเตอร์เพื่อคำนวณจุดจำกัดในการไหลสวนกันของของเหลวและก๊าซในท่อเอียง



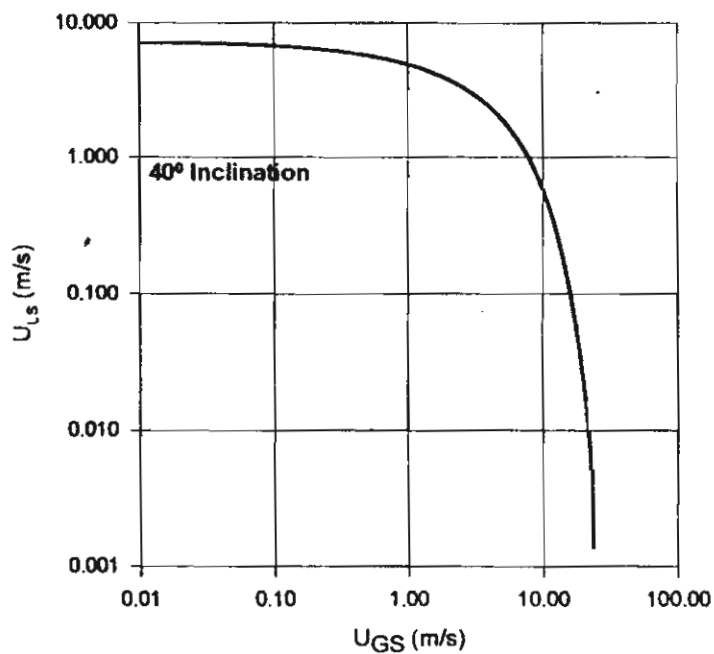
รูปที่ 3 แสดงจุดจำกัดในการไหลสวนกันของอากาศและน้ำในท่อขนาด $d = 0.051$ เมตร
ที่มุมเอียง 30 องศา



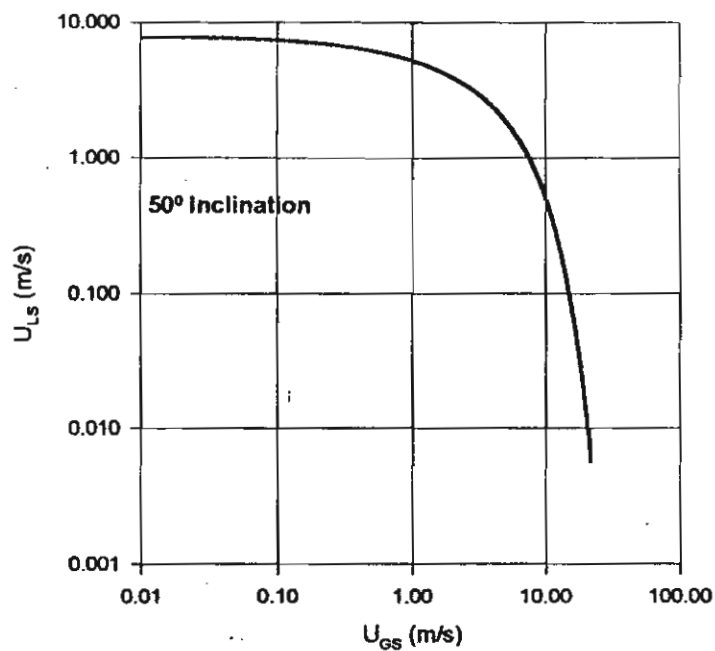
รูปที่ 4 แสดงจุดจำกัดในการไหลสวนกันของอากาศและน้ำในท่อขนาด $d = 0.051$ เมตร
ที่มุมเอียง 40 องศา



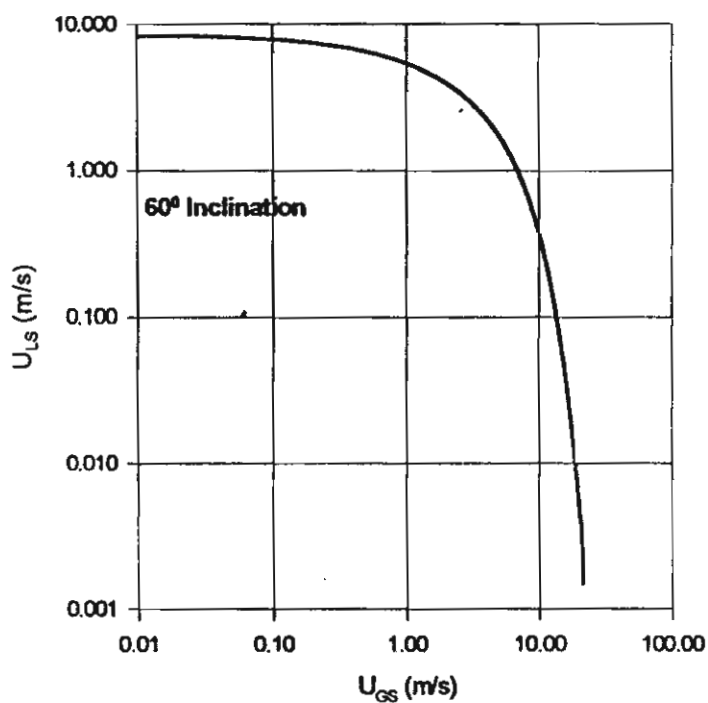
รูปที่ 3 แสดงจุดจำกัดในการไหลสวนกันของอากาศและน้ำในท่อขนาด $d = 0.051$ เมตร
ที่มุมเอียง 30 องศา



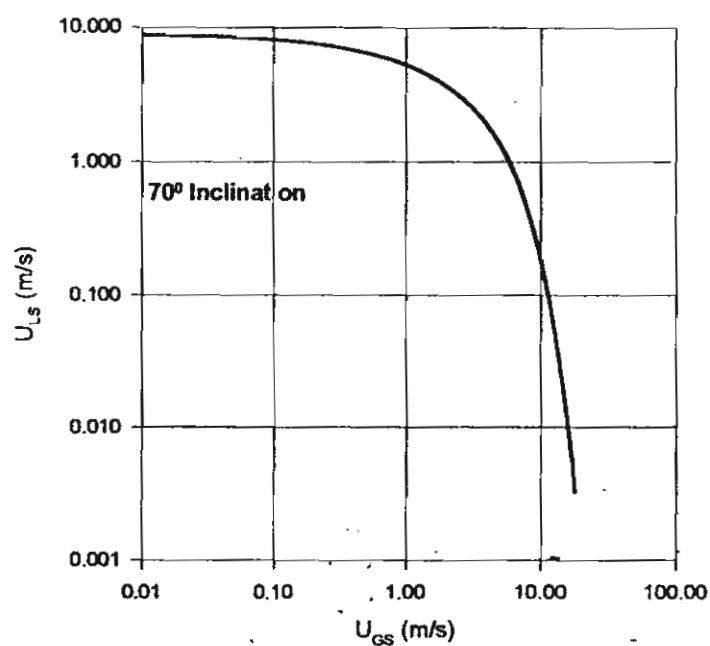
รูปที่ 4 แสดงจุดจำกัดในการไหลสวนกันของอากาศและน้ำในท่อขนาด $d = 0.051$ เมตร
ที่มุมเอียง 40 องศา



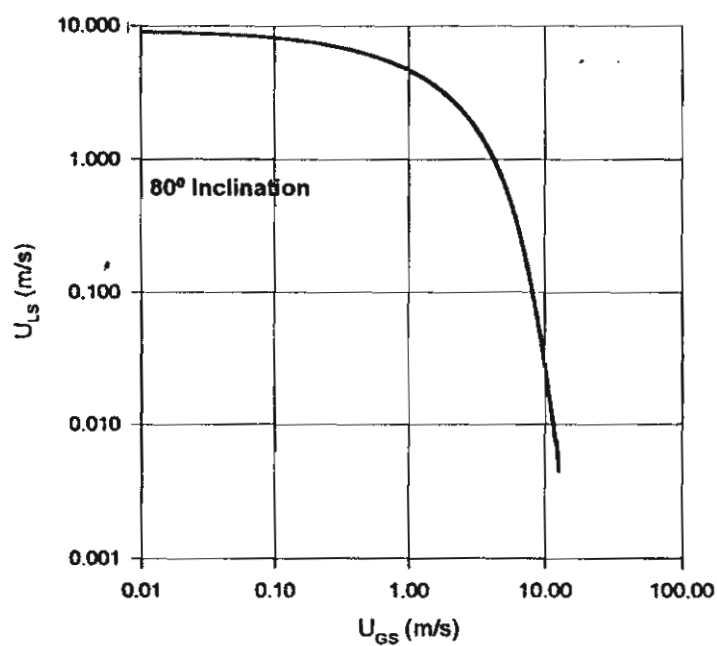
รูปที่ 5 แสดงจุดจำกัดในการไหลสวนกันของอากาศและน้ำในท่อขนาด $d = 0.051$ เมตร
ที่มุมเอียง 50 องศา



รูปที่ 6 แสดงจุดจำกัดในการไหลสวนกันของอากาศและน้ำในท่อขนาด $d = 0.051$ เมตร
ที่มุมเอียง 60 องศา

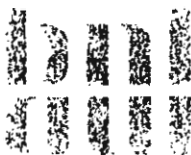


รูปที่ 7 แสดงจุดจำกัดในการไหลสวนกันของอากาศและน้ำในท่อขนาด $d = 0.051$ เมตร ที่มุมเอียง 70 องศา



รูปที่ 8 แสดงจุดจำกัดในการไหลสวนกันของอากาศและน้ำในท่อขนาด $d = 0.051$ เมตร ที่มุมเอียง 80 องศา

Wongwises, S., Method for prediction of pressure drop and liquid hold-up in horizontal stratified two-phase flow in pipes, *Proceedings of the 1997 ASME Symposium on Gas Liquid Two-Phase Flows*, June 22-26, 1997, Vancouver, Canada, pp. 1-7.



BROOKHAVEN NATIONAL LABORATORY
ASSOCIATED UNIVERSITIES, INC.

P.O. Box 5000
Upton, New York 11973-5000
TEL (516) 344- 2475
FAX (516) 344- 2613
E-MAIL rohatgi@bnl.gov

Department of Advanced Technology

January 13, 1997

Dr. Somchai Wongwises
Head of Fluid Mechanics Division
Department of Mechanical Engineering
King Mongkut Inst. Tech. Thonburi
Suksawad 48, Radburana,
Bangkok 10140, Thailand

Subject: Paper #GL-32/ "Method for Prediction of Pressure Drop and Liquid Hold-up in Horizontal Stratified Two-Phase Flows in Pipes"

Dear Sir:

I am happy to inform you that your paper has been reviewed and is accepted for the ASME International Symposium on Gas-Liquid Flow, June 22-26, 1997, Vancouver, Canada.

Enclosed are comments from reviewers which should be incorporated into your revised manuscript. ASME will directly send you instructions for a final form of the paper. The form and style will be similar to the ASME Journal of Fluids Engineering. The final version of the paper should be received here by February 28, 1997 to be included in the Symposium. In case you do not receive ASME instructions, follow the ASME Journal format and return the enclosed form (#1903) signed by all authors.

Thanks for contributing to the Symposium. Looking forward to seeing you in Vancouver, Canada.

Sincerely,

U.S. Rohatgi

U.S. Rohatgi
Symposium Organizer



ASME International

FLUIDS

ENGINEERING DIVISION

SUMMER MEETING

"The Annual ASME Fluids Engineering Conference & Exhibition"

Hyatt Regency Vancouver
Vancouver, British Columbia
June 22-26, 1997

FINAL PROGRAM

<http://www.asme.org>

- FEDSM97-3746 **Contributed Talk #1: Microgravity Two-Phase Flow: The State of the Art and Recent Progress**
K. Rezkallah, University of Saskatchewan
- FEDSM97-3747 **Contributed Talk #2: Particle Tracking and Ice Accretion in Turbine Engines**
D. W. Lankford, Sverdrup Technology, Inc. -- AEDC

2:00pm - 4:00pm

Tuesday, S242.7 / Room: Stanley

Sudden Expansion Flows

Chair: V. Otugen

- FEDSM97-3323 **Reynolds Number Asymptotic Covariance for Turbulent Pipe Flow Past a Sudden Expansion**
G. Papadopoulos, National Institute of Standards and Technology; Ioannis Lekakis, Universit of Thessaly; Franz Durst, Lehrstuhl fur Stromungsmechanik
- FEDSM97-3320 **Numerical Simulation of Laminar Pulsatile Flow in Axisymmetric Sudden Expansions**
R. K. Singh, S. Paquin, J.-M. Boy, A. Deslandes, S. Tavoularis, University of Ottawa
- FEDSM97-3307 **Control of Backward Facing Step Flow Using a Flapping Airfoil**
Joseph C. S. Lai, Jiannwoei Yue, Max F. Platzer, Naval Postgraduate School
- FEDSM97-3280 **High-Resolution, Unbiased LDV Measurements in the Flow Behind a Backwards-Facing Step**
Lance H. Benedict, Richard D. Gould, North Carolina State University
- FEDSM97-3279 **The Transport of Turbulent Kinetic Energy in the Flow Behind a Backwards-Facing Step**
Lance H. Benedict, Richard D. Gould, North Carolina State University
- FEDSM97-3316 **Turbulence Statistics of a Confined Swirling Flow**
Saad A. Ahmed, King Fahd University of Petroleum and Minerals

2:00pm - 4:00pm

Tuesday, S244.6 / Room: Oxford

Pipe Flows

Chairs: M. Shoukri
J. Bataille

- FEDSM97-3543 **Film Distribution for Gas-Liquid Flow in a Large Diameter Horizontal Pipe**
Leonid A. Dykhno, T. J. Hanratty, University of Illinois
- FEDSM97-3544 **The Effect of Branch Diameter on Two-Phase Pressure Drop and Phase Distribution at Horizontal Tee Junctions**
L. Walters, G. Sims, University of Manitoba; H.M. Soliman, AECL Research
- FEDSM97-3545 **Method for Prediction of Pressure Drop and Liquid Hold-Up in Horizontal Stratified Two-Phase Flow in Pipes**
Somchai Wongwises, King Mongkut Inst. Tech. Thonburi
- FEDSM97-3546 **The Flow of a Multiphase Fluid Through Piping**
Paul Morris, K. Hourigan, M. C Thompson, Monash University; S. A. T. Stoneman, University of Wales
- FEDSM97-3547 **The Rising of a Thin Film on the Vertical Wall Due to Thermocapillary Force**
F. Karibullina, F. Tazioukov, F. Garifoullin, P. Norden, Institute of Mechanical Engineering

2:00pm - 4:00pm

Tuesday, S245.6 / Room: Balmoral

Heat Transfer in Gas-Particle Flows

Chairs: Cill Richards
Alex Taylor

Method for Prediction of Pressure Drop and Liquid Hold-Up in Horizontal Stratified Two-Phase Flow in Pipes

S. WONGWISES

Department of Mechanical Engineering,
King Mongkut's Institute of Technology Thonburi
Bangmod, Bangkok 10140, Thailand

Abstract

Experimental apparatus was designed and constructed to obtain cocurrent air-water two phase flow in horizontal pipes. The test section, 10 m long, with an inside diameter 54 mm was made of transparent acrylic glass to permit visual observation of the flow patterns. The experiments were carried out under various air and water flow rates in the regime of smooth and wavy stratified flows. Stainless ring electrodes were mounted flush in the tube wall for measuring the liquid hold-up which is defined as the ratio of the cross-sectional area filled with liquid to the total cross-sectional area of the pipe. Calculation method for predicting the pressure drop and liquid hold-up was developed by using the Taitel and Dukler momentum balance between both phase. The ratio of interfacial friction factor and superficial gas-wall friction factor, (f_i/f_{SG}) was assumed to be constant. With this technique any mathematical model of interfacial friction factor is not necessary. A ratio of f_i/f_{SG} , which corresponds with the flow conditions, (laminar or turbulent) were presented.

Introduction

Analytical models have been developed for estimation of pressure drop in separated flow. Lockhart and Martinelli (1949) have developed a procedure for calculating the frictional pressure drop for adiabatic two-phase flow using their data on the horizontal flow of air and water and various other liquids at atmospheric pressure. The resulting correlations have been applied to all regions of two-phase flow both by the originators and by several other investigators, although the derivation is based on certain limiting assumptions. For some years, a team at CISE, Milan, Italy has been developing correlations for frictional pressure drop. Lombardi and Pedrocchi (1972) developed a general pressure drop correlation using CISE data. They employed consistent SI units for their correlations. Like Lockhart and Martinelli's pressure drop correlation, this correlation does not consider the effect of mass velocity. A wide variety of dimensionless groups have been used for correlating two-phase pressure drop. Another set of groups have been suggested by Kasturi and Stepanek (1972). They based their analysis on a separated flow model taking into account interactive effects by allowing the gas and liquid Reynolds numbers to affect respectively the liquid and gas friction factors. The original forms of the Martinelli model are known to be inaccurate and to give poor representation of the effects of system parameters, particularly of mass velocity. Chisholm (1978) has developed the Martinelli models in such a way that the

original Martinelli curves for the various flow regimes can be fitted quite well by selecting a fixed value of a parameter for each flow regime. Similar modifications have been made by Baker (1954) and by Chenoweth and Martin (1955). McMillan (1964) has also modified the Martinelli model by introducing a dimensionless parameter instead of using 0.046 for the calculation of the friction factor. Johannessen (1972) has developed a theoretical solution of the original Lockhart and Martinelli flow model for calculating two-phase pressure drop and holdup in the stratified and wavy flow region. He has shown that his theoretical solutions of pressure drop and holdup agree much better than those of Lockhart and Martinelli in the separated flow region. The phase-interaction models have been developed by Chawla (1972), Bandel and Schlunder (1974), Levy (1964), and Agrawal et al. (1973) independently. Although their physical models are believed to describe the processes involved, the accuracy of some of these pressure drop correlations, such as Chawla's and Levy's correlation is questionable.

The semi-empirical methods for two-phase flow pressure drop calculation have been proposed by numerous investigators. Wallis (1969) correlation which has been improved further by Hewitt and Hall-Taylor (1970) can be used in the annular flow region. Hughmark (1965) developed a semi-empirical pressure drop correlation independently which is applicable in slug flow region.

Baroczy (1966) proposed a general correlation for two-phase pressure drop. Although the correlation is

applicable to only a limited range of mass velocity, it predicts two-phase pressure drop fairly well within the range of mass velocity. He correlated the two-phase multiplier with a property index for various values of quality and mass velocity. Kadambi (1980) proposed an analytical procedure to determine the pressure drop and void fraction in two-phase stratified flow between parallel plates. Hart et al. (1989) used the interfacial friction factor of Eck (1973) to develop an ARS model for predicting the low values of the liquid holdup and values of the frictional pressure gradient.

Most stratified flow models were based on an iterative solution of the two phase momentum balance, but differed in the model of the interfacial shear stress. To solve this problem, Taitel and Dukler (1976) made the assumption that the interface was smooth and interfacial friction factor equal to the gas-wall friction factor and the gas interfacial shear stress was evaluated with the same equation as the gas wall shear stress. In their another paper (Taitel and Dukler (1976)), they demonstrated that the hold up and the dimensionless pressure drop for stratified flow are unique functions of X under the assumption that $f_G/f_L \equiv \text{constant}$. Kawaji (1987) predicted holdup successfully by substituting the ratio of the gas-wall friction factor and the gas interfacial shear stress into the Taitel and Dukler momentum balance. Spedding and Hand (1990) predicted the pressure loss and liquid holdup by assuming the ratio of the interfacial friction factor and gas-wall friction factor as a constant. The value of the constant depended on whether the phases were in turbulent or laminar flow. Their method will be modified for this study.

Experimental Apparatus and Method

A schematic diagram of the test facility is given in Fig 1. In the experimental investigations air and water were used as the working fluids. The main components of the system consisted of the test section, air supply, water supply, instrumentation, and data acquisition system.

The horizontal test section, with an inside diameter of 54 mm and length of 10 m was made of transparent acrylic glass to permit visual observation of the flow patterns. The connections of the piping system were designed such that parts could be changed very easily. Water was pumped from the storage tank through the rotameter to the water inlet section at the bottom of the pipe. Air was supplied to the test section by a suction-type blower. The air flow could be controlled by a valve at the outlet of the blower. Many small rods were used as guide vanes at the air inlet section to maintain a uniform flow. Both the air and water streams were brought together in a mixer and then passed through the test section cocurrently. The inlet flow rate of air was measured by means of a round-type orifice and that of water was measured by two sets of rotameters within a range of 0-4.8 m³/h. The temperature of air and water were measured by thermocouples ($\pm 0.5\%$). The two phase pressure drop between the test section was registered by a capacitive pressure transducer within the range of 0-1000 Pa ($\pm 5\%$). Stainless ring electrodes were mounted flush in the tube wall for measuring the liquid hold up, which was defined as the ratio of the cross-sectional area

filled with liquid to the total cross-sectional area of the pipe. The electrical conductivity of the water between the electrodes constituted an electrical resistance that could be registered, via a Wheatstone bridge, by a carrier frequency amplifier. The measured electrical resistance was a function of the electrode distance, the electrode width, and the level of the liquid between electrodes. The uncertainty in the measured liquid hold up was estimated to be $\pm 2\%$. All signals of the measuring transducers were registered by a data acquisition system with a frequency of 20 Hz, and finally they were averaged over the time elapsed.

Experiments were conducted with various flow rates of air and water at ambient condition. Average temperature in laboratory is about 30°C. In the experiments the air flow rate was increased by small increments while the water flow rate was kept constant at preselected value. After each change in inlet air flow rate, both the air and water flow rates were recorded. The liquid hold-up were registered through the transducers and transferred to the data acquisition system. The flow phenomena were detected by visual observation and sometime by camera.

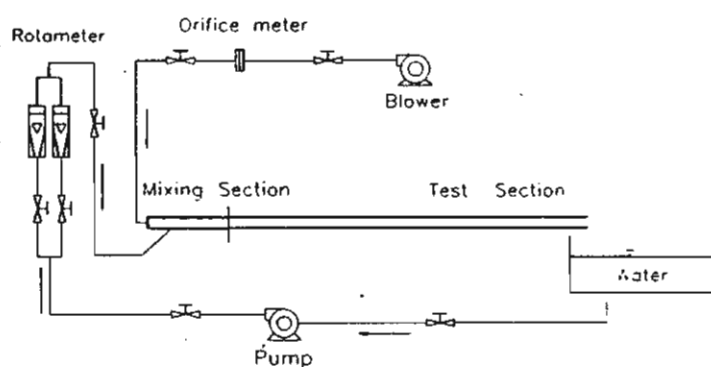


Figure 1 Schematic diagram of experimental apparatus

Theory

Consider a equilibrium horizontal stratified flow as shown in Fig. 2. A momentum balance on each phase yields:

$$-A_L \left(\frac{dP}{dx} \right) - \tau_{WL} S_L + \tau_i S_i = 0 \quad (1)$$

$$-A_G \left(\frac{dP}{dx} \right) - \tau_{WG} S_G - \tau_i S_i = 0 \quad (2)$$

Equating pressure drop in the two phases and assuming that the hydraulic gradient in the liquid is negligible, gives the following results

$$\tau_{WG} \frac{S_G}{A_G} - \tau_{WL} \frac{S_L}{A_L} + \tau_i S_i \left(\frac{1}{A_L} + \frac{1}{A_G} \right) = 0 \quad (3)$$

The shear stresses are evaluated in a conventional manner

$$\tau_{WL} = f_L \frac{\rho_L u_L^2}{2} \quad (4)$$

$$\tau_{WG} = f_G \frac{\rho_G u_G^2}{2} \quad (5)$$

$$\tau_i = f_i \frac{\rho_G (u_G - u_L)^2}{2} \quad (6)$$

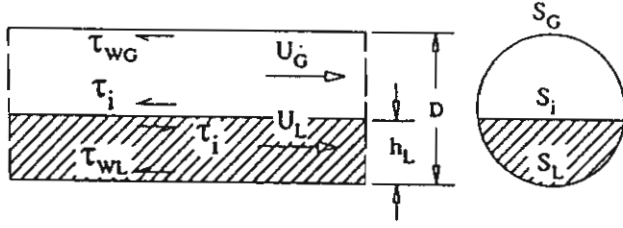


Figure 2 Stratified cocurrent flow

Normally for equilibrium flow $u_G \geq u_L$ such that u_L in eq.(6) can be neglected. A widely used method for the correlation of the liquid and gas friction factors is in the form of Blasius equation:

$$f_L = C_L \left(\frac{D_L u_L}{\nu_L} \right)^{-n} \quad (7)$$

$$f_G = C_G \left(\frac{D_G u_G}{\nu_G} \right)^{-m} \quad (8)$$

where D_L and D_G are the hydraulic diameter evaluated in the manner as suggested by Agrawal et al.(1973). The liquid is visualized as if it was flowing in an open channel .

$$D_L = \frac{4A_L}{S_L} \quad (9)$$

The gas is visualized as flowing in a closed duct and thus

$$D_G = \frac{4A_G}{S_G + S_i} \quad (10)$$

In this work the following coefficients are utilized: $C_G = C_L = 0.046, m = n = 0.20$ for the turbulent flow and $C_G = C_L = 16, m = n = 1.0$ for the laminar flow. Laminar flow is also assumed for superficial Reynold number < 2000 .

Substituting $\tau_{WL}, \tau_{WG}, \tau_i$ from Eq.(4), Eq.(5) and Eq.(6) into Eq.(3)

$$\begin{aligned} & \frac{f_G \rho_G u_G^2 S_G}{2A_G} - \frac{f_L \rho_L u_L^2 S_L}{2A_L} \\ & + \frac{f_i \rho_G u_G^2 S_i}{2} \left[\frac{1}{A_L} + \frac{1}{A_G} \right] = 0 \end{aligned} \quad (11)$$

for the single phase flow

$$\left(\frac{dP}{dx} \right)_{SG} = \frac{2f_{SG} \rho_G u_{SG}^2}{D} \quad (12)$$

To non-dimensionalize, Eq.(11) is divided by $\left(\frac{dP}{dx} \right)_{SG}$

$$\text{which } f_{SG} = C_G \left(\frac{D u_{SG}}{\nu_G} \right)^{-m}$$

$$\begin{aligned} & \frac{f_G u_G^2 S_G D}{4f_{SG} A_G u_{SG}^2} - \frac{f_L \rho_L u_L^2 S_L D}{4f_{SG} \rho_G A_L u_{SG}^2} \\ & + \frac{f_i \rho_G u_G^2 S_i D}{4f_{SG} \rho_G u_{SG}^2} \left[\frac{1}{A_L} + \frac{1}{A_G} \right] = 0 \end{aligned} \quad (13)$$

or in dimensionless form

$$\begin{aligned} & (\bar{u}_G)^2 (\bar{D}_G \bar{u}_G)^{-m} \frac{\bar{S}_G}{\bar{A}_G} - \left[(\bar{u}_L)^2 (\bar{D}_L \bar{u}_L)^{-n} \frac{\bar{S}_L}{\bar{A}_L} \right] X^2 \\ & + \frac{f_i}{f_{SG}} (\bar{u}_G)^2 \left[\frac{\bar{S}_i}{\bar{A}_L} + \frac{\bar{S}_i}{\bar{A}_G} \right] = 0 \end{aligned} \quad (14)$$

which $X^2 = (dP/dx)_{SL} / (dP/dx)_{SG}$ is the ratio of the frictional pressure gradient of the liquid to that of the gas when each phase flows along in the pipe.

$$X^2 = \frac{\frac{4C_L}{D} \left(\frac{u_{SL} D}{\nu_L} \right)^{-n} \frac{\rho_L (u_{SL})^2}{2}}{\frac{4C_G}{D} \left(\frac{u_{SG} D}{\nu_G} \right)^{-m} \frac{\rho_G (u_{SG})^2}{2}} \quad (15)$$

X is recognized as the parameter introduced by Lockhart and Martinelli (1949) and can be calculated unambiguously with the knowledge of the flow rate, fluid properties and tube diameter. Liquid hold up can be calculated from h_L/D which is in form of \bar{A}_G, \bar{A}_L .

All dimensionless variables with the superscript can be seen from

$$\tilde{A} = \pi/4, \quad \tilde{A}_L = A_L/D^2, \quad \tilde{S}_L = S_L/D$$

$$\tilde{A}_G = A_G/D^2, \quad \tilde{S}_G = S_G/D, \quad \tilde{S}_i = S_i/D$$

$$\tilde{D}_L = D_L/D, \quad \tilde{D}_G = D_G/D, \quad \tilde{h}_L = h_L/D$$

$$\tilde{S}_L = \pi - \cos^{-1}(2\tilde{h}_L - 1), \quad \tilde{S}_G = \cos^{-1}(2\tilde{h}_L - 1),$$

$$\tilde{S}_i = \sqrt{1 - (2\tilde{h}_L - 1)^2}, \quad \tilde{U}_G = \frac{\tilde{A}}{\tilde{A}_G}, \quad \tilde{U}_L = \frac{\tilde{A}}{\tilde{A}_L}$$

$$\tilde{A}_L = 0.25 \left[\pi - \cos^{-1}(2\tilde{h}_L - 1) + (2\tilde{h}_L - 1) \sqrt{1 - (2\tilde{h}_L - 1)^2} \right]$$

$$\tilde{A}_G = 0.25 \left[\cos^{-1}(2\tilde{h}_L - 1) - (2\tilde{h}_L - 1) \sqrt{1 - (2\tilde{h}_L - 1)^2} \right]$$

In order to solve Eq.(14) for liquid hold up, gas hold up and pressure drop, an iterative computer program is required. A flow chart of this program is shown in Fig 3.

Results and Discussion

Visual observation shows that different flow patterns may occur with gas-liquid cocurrent flow in horizontal pipes. In accordance with results obtained from this experiment, the following flow patterns were obtained :

a) Stratified flow: The water flows in the lower part of the pipe and the air over it with a smooth interface between the two phases.

b) Two-dimensional wavy flow: Similar to stratified flow except for a wavy interface, due to a velocity difference between the two phases and two-dimensional steady waves travel with a relatively regular pitch.

c) Three-dimensional wavy flow: At a higher air flow rate, the water surface is disturbed and three-dimensional waves occur, which have small irregular ripples on the fundamental waves.

d) Semi-slug flow: The semi-slug is defined as a highly agitated long wave which contains many bubbles. Its upstream and downstream portions are similar to the wavy flow.

e) Slug flow: Splashes or slugs of water occasionally pass through the pipe with a higher velocity than the bulk of the water. The tail of water slug is relatively smooth and sometimes contains some small bubbles. The upstream portion of the water slug is similar to the wavy flow, and the downstream portion to the stratified flow or wavy flow.

f) Plug flow: Air moves along the upperside of the pipe. This flow pattern occurs at a relatively low air flow rate. The interface is smooth and no bubbles are contained in a water plug.

g) Violent wavy flow: The interface is violently disturbed by the air stream. This flow pattern occurs at a relatively high air flow rate.

The typical photographs of flow patterns are shown in Figure 4.

The focus of the study was on the stratified and wavy flow. Figures 5 and 6 shows the relation between the liquid holdup, ϵ_L against the Lockhart-Martinelli parameter, X for a laminar liquid-turbulent gas flow in the 0.054 m. diameter

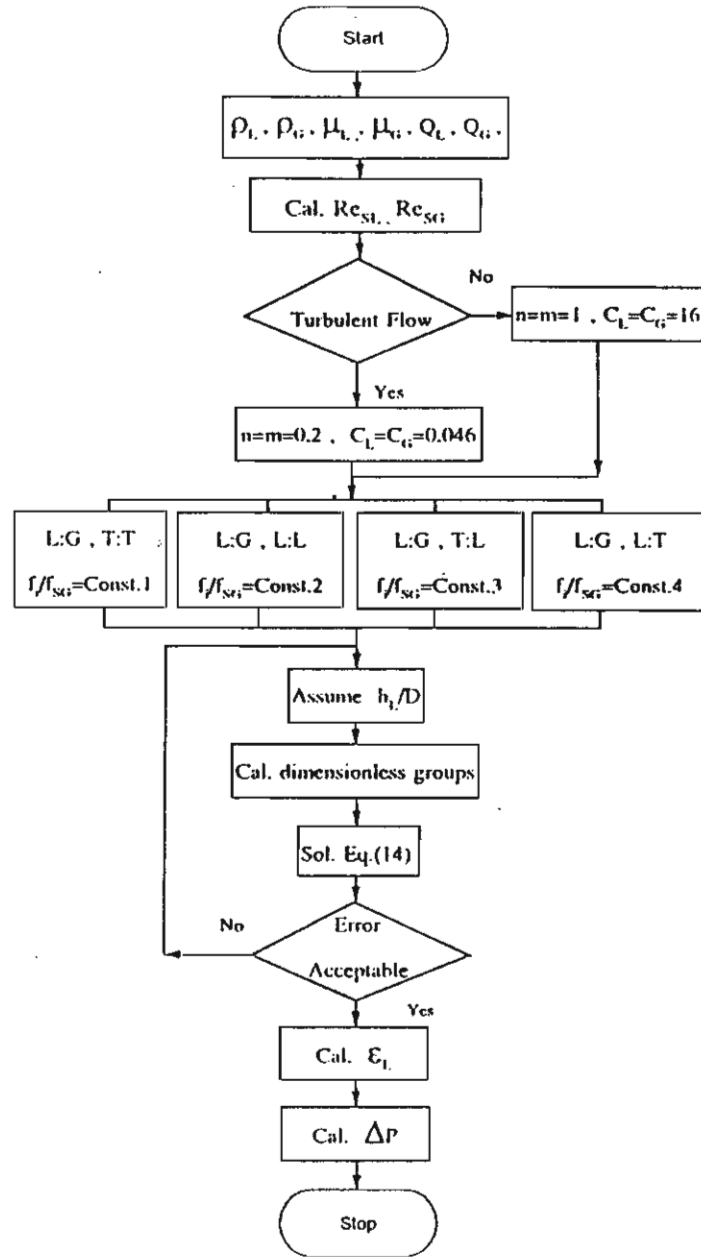
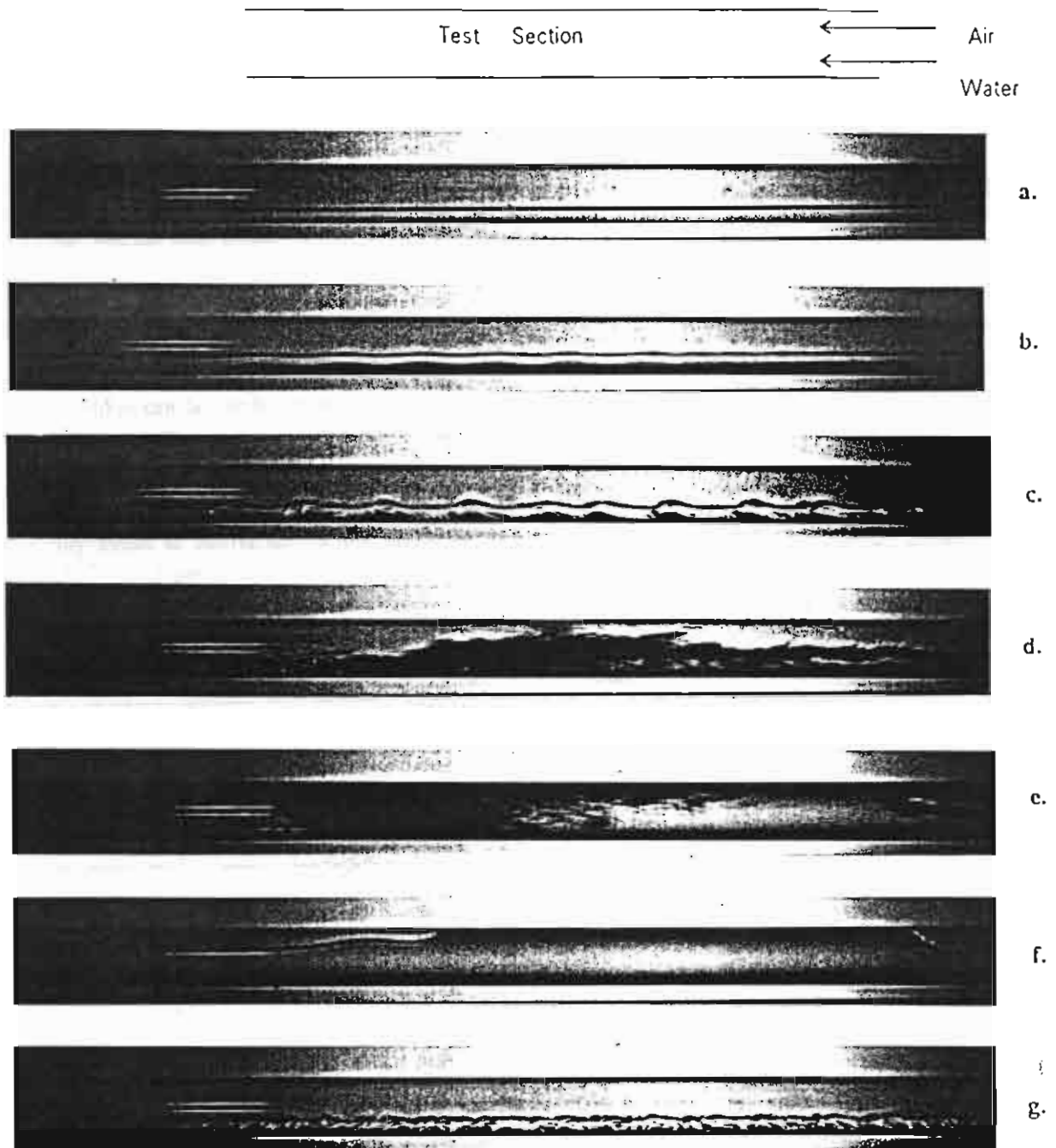


Figure 3 Flow chart of liquid hold-up and pressure drop calculation

pipe and $Q_{L1} = 1.67 \times 10^{-5}$, 6.67×10^{-5} m³/s respectively. The values $C_G=C_L=0.046$, $n=m=0.2$ for turbulent flow and $C_G=C_L=16$, $n=m=1.0$ for laminar flow are used. The figures show a comparison of the experimental data with the present model which the ratio, f/f_{SG} are assumed. It is found that an agreement of the present model with the experimental data is obtained by using $f/f_{SG} = 0.30-1.0$. Figures 7 and 8 show also the relation between ϵ_L against X for a turbulent liquid - turbulent gas flow for $Q_{L1}=8.3 \times 10^{-5}$, 1.67×10^{-4} m³/s respectively. They show that the air-water liquid holdup can be accurately predicted by assuming $f/f_{SG} = 2.0-4.0$. The data



- | | |
|--------------------------------|----------------------|
| a. Stratified Flow | e. Slug Flow |
| b. Two-Dimensional Wavy Flow | f. Plug Flow |
| c. Three-Dimensional Wavy Flow | g. Violent Wavy Flow |
| d. Semi-Slug Flow | |

Figure 4. Photographs of flow patterns

shows that the assumption of $f_i/f_{SG} = 1.0$ overpredicted liquid holdup for the stratified flows. The results correspond to those from Spedding et al. (1990) who tested the model against wavy and stratified flow data from 93.5 and 45.5 mm i.d. pipes. The data can be accurately predicted with $f_i/f_{SG} = 0.6$ and $f_i/f_{SG} = 4$ for laminar liquid-turbulent gas flow and turbulent liquid-turbulent gas flow respectively. Their predicted f_i/f_{SG} are in the recommended interval in this work. Two-phase pressure drop can be determined by substituting h_i/D into Eq. (1) or (2). In this work, the situations when gas flow was laminar, was not considered.

Conclusion

This paper presents new data to predict the liquid holdup and pressure drop in horizontal cocurrent stratified flow in a circular pipe. It has been demonstrated that the pressure drop and the liquid holdup can be predicted by using Taitel and Dukler momentum balance between both phase. The ratio of the friction factor of the gas at the interface and the gas at the pipe wall, f_i/f_{SG} is assumed to be constant. The constant depends on the phase being either turbulent or laminar. With this method any model of interfacial friction factor is not necessary. For turbulent liquid-turbulent gas flows, the former assumption that $f_i = f_{SG}$ is shown to give a result which does not agree with the experimental data.

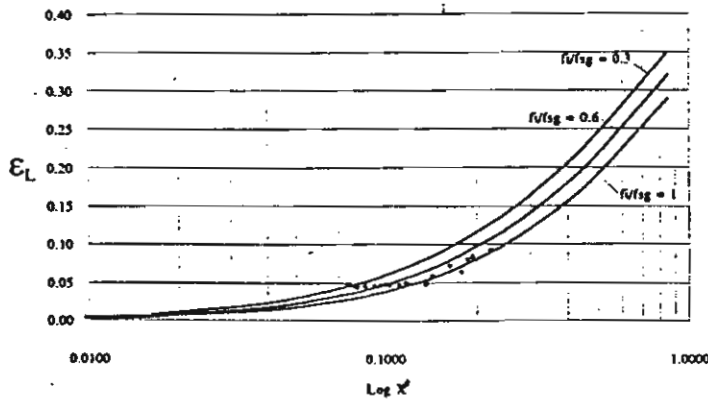


Figure 5. Experimental data obtained from a water rate = $1.667 \times 10^{-5} \text{ m}^3/\text{s}$
Liquid - Laminar and Gas - Turbulent

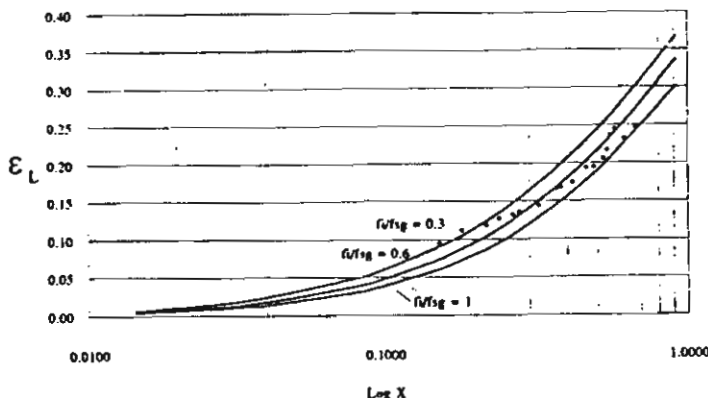


Figure 6. Experimental data obtained from a water rate = $6.67 \times 10^{-5} \text{ m}^3/\text{s}$
Liquid - Laminar and Gas - Turbulent

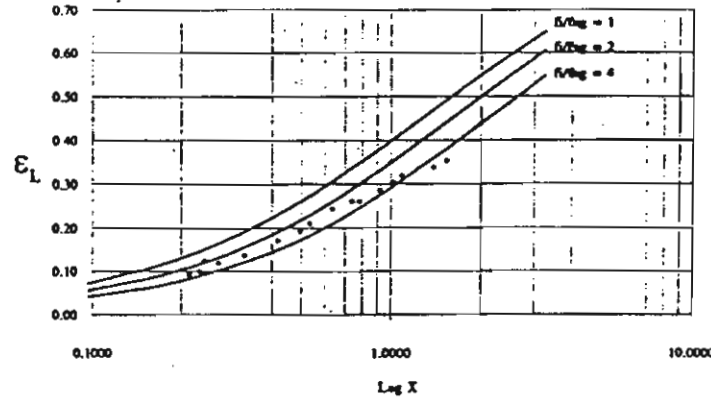


Figure 7. Experimental data obtained from a water rate = $8.33 \times 10^{-5} \text{ m}^3/\text{s}$
Liquid - Turbulent and Gas - Turbulent

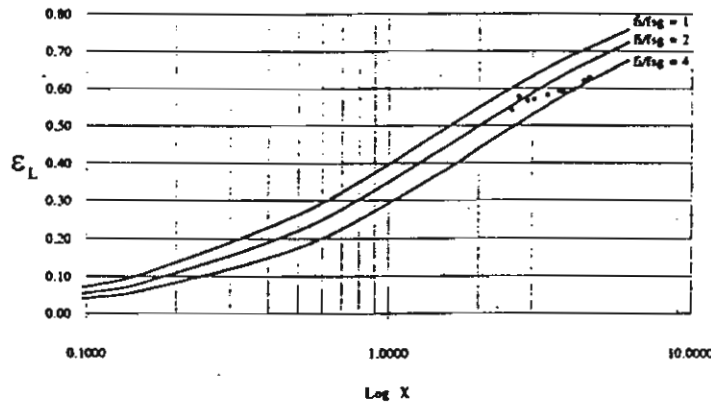


Figure 8. Experimental data obtained from a water rate = $1.67 \times 10^{-4} \text{ m}^3/\text{s}$
Liquid - Turbulent and Gas - Turbulent

Nomenclature

A	Crosssectional area of pipe, m^2
A_G, A_L	Crosssectional area of gas and liquid phase, m^2
C_G, C_L	Constant in Eq. (7) and (8)
D	Pipe diameter, m
D_G, D_L	Hydraulic diameter of gas and liquid phase, m
f_G, f_L	Gas-wall and liquid-wall friction factor
f_i	Interfacial friction factor
f_{SG}	Superficial gas-wall friction factor
g	Gravitational acceleration, m/s^2
h	Liquid height, m
n, m	Constant in Eq. (7) and (8)
P	Pressure, N/m^2
dP/dx	Two phase pressure gradient, N/m^3
$(dP/dx)_{SG}$	Pressure gradient of single gas phase. N/m^3
$(dP/dx)_{SL}$	Pressure gradient of single liquid phase. N/m^3
Q_G	Volume flow rate of gas, m^3/s
Q_L	Volume flow rate of liquid, m^3/s
Re_G	Gas phase Reynolds number
Re_L	Liquid phase Reynolds number

Re_{SG}	Superficial gas phase Reynolds number
Re_{SL}	Superficial liquid phase Reynolds number
S_G	Gas phase perimeter, m
S_L	Liquid phase perimeter, m
S_i	Interfacial width, m
U_G	Average velocity of gas, m/s
U_L	Average velocity of liquid, m/s
U_{SG}	Superficial velocity of gas, m/s
U_{SL}	Superficial velocity of liquid, m/s
X	Lockhart-Martinelli parameter

Greek Symbols

ρ	Density, kg/m ³
ν	Kinematic viscosity, m ² /s
τ	Shear Stress, N/m ²
ϵ	Hold up

Subscripts

G	Gas phase
L	Liquid phase
i	Interface
WL	Liquid-wall
WG	Gas-wall
SG	Superficial gas
SL	Superficial liquid

Superscripts

~	dimensionless term
---	--------------------

Acknowledgement

This work was given financial support by the Thailand Research Fund, whose guidance and assistance are gratefully acknowledged.

References

- Agrawal, S.S., Gregory G.A., and Govier G.W., 1973, "An Analysis of Horizontal Stratified Two Phase Flow in Pipes", *Can J. Chem. Eng.*, Vol. 51, pp.280-286.
- Baker, O., 1954, "Simultaneous Flow of Oil and Gas" *Oil and Gas J.*, Vol. 53, pp.185-195.
- Bandel, J., and Schlunder, E.U., 1974, "Frictional Pressure Drop and Convective Heat Transfer of Gas-Liquid Flow in Horizontal Tubes", *Int. Centre Heat and Mass Transfer, Int. Heat Transfer Conf. Proc.* Vol.5, pp.190-194.
- Baroczy, C.J., 1996, "A Systematic Correlation for Two-Phase Pressure Drop," *NACA-SR-Memo-11858*, North American Aviation.
- Chawla, J.M., 1972, "Frictional Pressure Drop in the Flow of Liquid/Gas Mixtures in Horizontal Pipes", *Chem. Ing. Tech.* 44, pp.58-62.
- Chenoweth, J.M., and Martin, M.W., 1955, "Turbulent Two Phase Flow", *Pet. Ref.*, Vol.34, pp.151-155.
- Chisholm, D., 1978, "Influence of Pipe Surface Roughness on Friction Pressure Gradient During Two Phase Flow", *Mech. Eng. Sci.* Vol. 20, pp.353-354.
- Dukler, A.E., Wicks, M. and Cleveland, R.G., 1964, "Frictional Pressure Drop in Two Phase Flow: An Approach Through Similarity Analysis", *AIChE*, Vol. 10, pp.44-51.
- Eck, B., 1973, *Technische Stromungslehre*, Springer, New York.
- Hart, J., Hamersma, P.J. and Fortuin, J.M., 1989, "Correlations Predicting Frictional Pressure Drop and Liquid Holdup During Horizontal Gas-Liquid Pipe Flow with a Small Liquid Holdup", *Int. J. Multiphase Flow*, Vol. 15, pp. 947-964.
- Hewitt, G.F. and Hall-Taylor, N.W., 1970, *Annular Two-Phase Flow*, Pergamon Press.
- Hughmark, G.A., 1965, "Holdup and Heat Transfer in Horizontal Slug Gas-Liquid Flow", *Chem. Eng. Sci.*, Vol.20, pp. 1007-1010.
- Johannessen, T., 1972, "A Theoretical Solution of the Lockhart-Martinelli Flow Model to Calculate Two Phase Flow Pressure Drop and Holdup", *Int. J. Heat Mass Transfer*, Vol. 15, pp.1443-1449.
- Kadambi, V., 1980, "Prediction of Void Fraction and Pressure Drop in Two-Phase Annular Flow", GE Rep. No. 80 CRD156.
- Kasturi, G. and Stepanek, J.B., 1972, *Chem. Eng. Sci.*, Vol.27, pp. 1871.
- Kawaji, M., Anoda, Y., Nakamura, H. and Tasaka, T., 1987, "Phase and Velocity Distributions and Holdup in High-Pressure Steam/Water Stratified Flow in a Large Diameter Horizontal Pipe", *Int. J. Multiphase Flow*, Vol.13, pp.145-159.
- Levy, S., 1964, "Analysis of Various Types of Two-Phase Annular Flow, Part II - Prediction of Two-Phase Annular Flow with Liquid Entrainment," GEAP-4615.
- Lockhart, R.W. and Martinelli, R.C., 1949, "Proposed Correlation of Data for Isothermal Two Phase, Two Component Flow in Pipes, *Chem. Engg. Prog.* Vol.45, pp.39-48.
- Lombardi, E. and Pedrochi, E., "Pressure Drop Correlation in Two-Phase Flow", *Energ. Nucl.* 19, 1972, pp. 91-99.
- McMillan, H.K., 1964, "A Study of Flow Pattern and Pressure Drop in Horizontal Two-Phase Flow", Ph.D. Thesis, Purdue University.
- Spedding, P.L. and Chen, J.J.J., 1984, "Holdup in Two-Phase Flow", *Int. J. Multiphase Flow*, Vol.10, pp.307-339.
- Spedding, P.L. and Hand, N.P., 1990, "Prediction of Holdup and Pressure Loss from the Two Phase Momentum Balance for Stratified Type Flows, in *Advances in Gas-Liquid Flow*, FED-Vol.99, HTF-Vol.155, pp.221-228.
- Taitel, Y., and Dukler, A.E., 1976, "A Model for Predicting Flow Regime Transitions in Horizontal and Near Horizontal Gas-Liquid Flow", *AIChE*, Vol.22, pp.47-55.
- Taitel, Y., and Dukler, A.E., 1976, "A Theoretical Approach to the Lockhart-Martinelli Correlation for Stratified Flow", *Int. J. Multiphase Flow*, Vol. 2, pp. 591-595.
- Wallis, G.B., 1969, *One-Dimensional Two-Phase Flow*, McGraw-Hill Book Co., New York.

Kalinitchenko, V.A., **Wongwises, S.**, On the structure of free surface flow over complex topographic features, *Proceedings of the 1997 ASME Fluids Engineering Conference & Exhibition*, June 22-26, 1997, Vancouver, Canada, pp. 1-6.



ASME International

FLUIDS

ENGINEERING DIVISION

SUMMER MEETING

"The Annual ASME Fluids Engineering Conference & Exhibition"

Hyatt Regency Vancouver
Vancouver, British Columbia
June 22-26, 1997

FINAL PROGRAM

<http://www.asme.org>

- FEDSM97-3632 **Centrifuging Effects on Pulverized Coal Particles in a Gas-Piloted Swirl-Stabilised Flame**
Y. Hardalupas, Ilias Prassas, J. Whitelaw, Imperial College of Science Tech. & Medicine
- FEDSM97-3604 **An Experimental Study of Swirling Gas-Particle Flow in a Vertical Pipeline**
Hui Li, Kagoshima University; Yugi Tomita, Kyushu Institute of Technology

2:00pm - 4:00pm

Thursday, G12.4 / Room: Plaza East

Flow Devices and Applications

Chairs: John Baker, University of Alabama, Birmingham

Frank M. White, University of Rhode Island

- FEDSM97-3028 **Pressure Drop in Metal Matrices for High Gradient Magnetic Separation**
G. F. Jones, Villanova University; F. C. Prenger, P. M. Williams, M. A. White, Los Alamos National Laboratory
- FEDSM97-3033 **Measurements of Added Mass and Damping on Hydraulic Gate Models**
C. Knisely, G. Klein, Bucknell Univ.; N. Ishii, Osaka Electro-Communications University
- FEDSM97-3035 **High Perf. Spiral Air-Flow Apparatus for Purging Residual Water in a Pipeline**
Kiyoshi Horii, Shirayuri Women's College; Yao-Hua Zhao, Kyushu University; Yuji Tomita, Kyushu Institute of Technology; Yukio Shimo, NTT Science and Core Tech. Lab.
- FEDSM97-3042 **On the Structure of Free Surface Flow Over Complex Topographic Features**
Vladimir A. Kalinitchenko, Russian Academy of Sciences; Somchai Wongwises, King Mongkut Inst. of Technology
- FEDSM97-3044 **On the Influence of Wall Properties in Peristaltic Transport of Particle-Fluid Suspension**
R. Usha, K. Prema, Indian Institute of Technology

2:00pm - 4:00pm

Thursday, F162.3 / Room: Regency West

Aerodynamic and Surface Configurations

Chairs: Brian E. Thompson, Rensselaer Polytechnic Institute

L. Patrick Purtell, Office of Naval Research

- FEDSM97-3135 **Recirculating Wakes of Snow-Plowing Vehicles**
Brian E. Thompson, Rensselaer Polytechnic Institute; Hany K. Nakhla, Rensselaer Polytechnic Institute
- FEDSM97-3136 **Aerodynamic Behavior of Wave Transients in Railway Tunnels by Two High-Speed Trains**
Walter Gretler, Technical University of Graz
- FEDSM97-3137 **Numerical Study of Compression Wave Produced by High-Speed Train Entering a Tunnel**
Wam-Gyu Park, Pusan National University; Young-Joon Park, Pusan National University; Seong-Do Ha, Korea Institute of Machinery and Materials
- FEDSM97-3138 **Aerodynamic Efficiency of Speed-Skier Configurations**
W. A. Friess, Rensselaer Polytechnic Institute; K. N. Knapp II, Rensselaer Polytechnic Institute; B.E. Thompson, Rensselaer Polytechnic Institute; M. Skakel, Rensselaer Polytechnic Institute
- FEDSM97-3139 **Thoughts on the Use of Commercial RANS Code for Sailing Yacht Design**
W. Lasher, Pennsylvania State University; Paul Zonneveld, Pennsylvania State University

2:00pm - 4:00pm

Thursday, F166.7 / Room: Peacocks

Cavitation-Modelling and Damage

Chairs: Joseph Katz

Kevin Farrell

FEDSM97-3042

ON THE STRUCTURE OF FREE SURFACE FLOW OVER COMPLEX TOPOGRAPHIC FEATURES

Vladimir A. KALINITCHENKO

Lab. of Wave Processes, Inst. for Problems
in Mechanics, Russian Academy of Sciences,
pr. Vernadskogo, 101 Moscow, 117526 RUSSIA
Fax: 7-095-938-2048
Email: kalin@ipm.msk.su

Somchai WONGWISES

Dept. of Mechanical Engineering,
King Mongkut's Inst. of Technology Thonburi,
Suksawad 48 Rd., Bangkok 10140 THAILAND
Fax: 662-427-8787
Email: isomises@cc.kmit.ac.th

ABSTRACT

This paper concerns analysis of steady flow in channels having irregularities of an idealized periodic form. An analytic model of non-separating potential flow above an impermeable wavy bed is used to investigate the free surface elevation and the velocity field. It is shown that the effect of bottom undulations depends on their steepness. The generalization of results based on linear theory is achieved by the use of Fourier series, resulting in the examination of a more complex bottom forms. The results of experiments in the open channel flume regarding the development of the mean and fluctuating flow field are analyzed in detail in the case of a sinusoidal bottom of different steepness, 'sawtooth bed' under various current conditions.

1. INTRODUCTION.

The dynamics of the water-sediment interface have received much attention in recent years, especially mechanisms governing the interaction between fluid flow and bottom materials. The motion of a given bed material in a given channel depends entirely on the mechanical structure of the flow which generates this sediment motion. On the other hand, observations showed that the motion of the sediment is accompanied by certain features of its own, such as the wavelike deformation of the bottom surface and the diffusion of solid particles into the fluid. Bedforms play a significant role in the makeup of resistance to flow in alluvial channels, and many engineering problems associated with coastal environment are often determined by sediment transport due to current and wave

action. An understanding of the generation and properties of bed forms can be expected from detailed analysis of the kinematics and dynamics of the interaction between flow and the bed.

The nature of the flow over a movable sediment bed has been subject of a variety of theoretical and experimental investigations. It is worth noting works of Kennedy (1963,1969), Reynolds (1965), Davies (1979,1983), Longuet-Higgins (1981), Van Rijn et al (1993), Mel'nikova (1996) and others.

The Kennedy-Reynolds model predicts bed forms, their characteristics, and their stability for a free surface flow over an erodible bed. In the case of zero lags between the local sediment transport and the local velocity of fluid the dominant wavelength of the bed two-dimensional form can be determined from

$$F^2 = U^2 / (gh) = (2 + kh \tanh kh) / [(kh)^2 + 3 kh \tanh kh] \quad (1)$$

where F is the Froude number, U is the velocity of uniform flow, g is the acceleration due to gravity, k is the wavenumber, h is the fluid depth. Experiments showed that for certain intervals of the Froude number, the surface of a mobile bed had periodic irregularities - sandwaves. Note that the Kennedy-Reynolds' model is not totally realistic because it ignores the separation zone associated with bed forms, and no generally accepted theory of the origin of sand waves has been produced. Fluid flowing over a bottom undulation separates somewhere on the downstream side of the crest, reattaching on the upstream face of the next crest. This would cause a pressure asymmetry with respect to the crest resulting in bedform growth.

The analysis of real turbulent flows over erodible beds requires the experimental results and theoretical models of single-phase turbulent flows over impermeable bottom structures. This approach closely approximates to the real situation since the celerity of the bedforms' movement is small compared to the fluid velocity.

Davies (1979,1983) derived the model describing uniform and wave-induced flows over impermeable rippled surface which were simulated by superimposing irrotational flow solutions: uniform flow or oscillations in the horizontal direction is perturbed by introducing a repeated pattern of discrete singularities, such that one of the streamlines of the resulting motion is distorted into desired ripple shape.

Having considered different sediments forms on the beds of alluvial channels, Mercer and Haque (1973) developed the model based on potential flow over a linearized boundary composed of a periodic series of modified wedges and eddy shear lines. In their experiments on flow over undulated Styrofoam beds velocity measurements made with a static-pitot tube showed a positive velocity gradient along the wedge.

Ranasoma and Sleath (1994) have described LDA-measurements of the fluid velocities in a steady-flow recirculating flume with a section of the bed that could be oscillated at right angles to the steady flow. The combined flow time-mean velocity profiles showed reasonable agreement with an eddy viscosity model at large distances from the bed, but not-as-good agreement very close to the bed. It was suggested that the discrepancies between theory and experiment in the immediate vicinity of the bed are due to the large scale momentum exchanges caused by vortex formation.

Accurate kinematics in the fluid domain are needed for the determination of physically realistic models for the estimation of shear stresses on the bed. At the moment there is no universally accepted method for the accurate calculation of flow-sediment interaction and sediment transport. As a consequence, all theories have to be calibrated and tested against measurements. Unfortunately, very few accurate flow kinematics measurements exist in the crest-to-trough region of bottom undulations.

The considerations in this paper are confined to the study of uniform or quasi-uniform flows only which can be treated as two-dimensional. The experiments were carried out in a flume with an undulated bottom using a laser Doppler anemometer (LDA) to obtain velocity profiles. Research concentrated on the bottom crest and trough regions and covered a number of different flow and bottom undulation conditions.

2. MODEL: STEADY-STATE FLOW OVER AN UNDULATED BOTTOM

Assume that the fluid is of depth h and has flow velocity U in the positive x -direction. The bed is impermeable and undulated infinitely, and the flow nonseparating. Let the

function $y = -h + \eta(x)$ describe the bedform, where $\eta(x) = a \cos kx$ and a is small.

In this analysis the form of the bed and free surface will be idealized as two-dimensional. The flow will be treated as irrotational, and the viscosity, surface tension, and the compressibility of the fluid will be neglected. The velocity v can be expressed as the gradient of a velocity potential ϕ which must represent the uniform current U and a small perturbed motion of fluid:

$$v = (U + u, v) = -\text{grad } \phi$$

where u and v are velocity components of the fluid motion, and ϕ is the sum of the velocity potential ($-Ux$) existing in the absence of bottom undulations and the perturbation ϕ^* .

If the displacement of the fluid free surface is ζ , the linear boundary problem is as follows

$$\Delta \phi^* = 0 \quad \text{at } -h \leq y \leq 0 \quad (2)$$

$$-\phi^*_{,x} \zeta_x + \phi^*_{,y} = 0 \quad \text{on } y = 0 \quad (3)$$

$$g \zeta + U \phi^*_{,x} = 0 \quad \text{on } y = 0 \quad (4)$$

$$-U \eta_x + \phi^*_{,y} = 0 \quad \text{on } y = -h \quad (5)$$

where subscripts denote differentiation.

The velocity potential is expressed by

$$\phi = -Ux + \frac{aU^3}{2k \cosh kh} \left[\left(-\frac{g}{U^2} + k \right) e^{ky} - \left(\frac{g}{U^2} - k \right) e^{-ky} \right] \frac{\sin kx}{U^2 - c^2} \quad (6)$$

where c is the celerity of waves of length $L = 2\pi/k$ in water of depth h

$$c^2 = g/k \tanh kh \quad (7)$$

The equation of free surface is

$$\zeta = aU^2 \cos kx / [\cosh kh (U^2 - c^2)] \quad (8)$$

Thus the crests and troughs of the free surface and the bottom correspond or are opposite according as

$$U^2 > c^2 \quad \text{or} \quad U^2 < c^2$$

For deep water the horizontal velocities at the crest and trough positions on the bed surface, u_{cr} and u_{tr} , are given by

$$u_{cr/tr} = U(1 \pm ak) \quad (9)$$

and so depend directly on the undulated bottom steepness ak .

The stream function $\psi(x,y)$ is determined by

$$\psi = -Uy + \frac{dU^3}{2k \cos h kh} \left[\left(\frac{g}{U^2} + k \right) e^{ky} - \left(\frac{g}{U^2} - k \right) e^{-ky} \right] \frac{\cos kx}{U^2 - c^2} \quad (10)$$

Note that any bed profile that is a simple harmonic function of x can be obtained by linear superposition of expression of the form $\eta_n(x) = a_n \cos k_n x$ since it is the most general Fourier component. Even though, in any particular case, the coefficients in the series may be small, their effect on the flow near the bed may be large since the effect of the bottom undulations depends not on their amplitudes, but on their steepnesses.

3. EXPERIMENTAL PROCEDURES

The measurements were made in a steady-flow recirculating flume which had a total length of 160 cm, a width of 8 cm, and a depth of 14 cm. The current was generated by a constant head system. By adjusting the height of the weir at the end of the flume, the desired water depth was obtained.

Two types of sediment material were used: sand with diameters of 0.35 mm and 0.60 mm. The mean diameter of sand particles was determined by the standard range particle size analyzer MICROTRACII utilizing the phenomenon of low-angle forward scattered light from a laser beam projected through stream particle.

The modeling clay was used to produce the undulated rigid bottom forms, which were symmetrical about their crests in the horizontal direction. The undulated section of bed was 100 cm long. The flow took place over the section of undulations of identical sinusoidal or triangular shape and size. The steepness ak was varied through the range from 0.15 to 0.63.

The procedure in the experiments was to measure the velocity in the free stream flow using volumetric method and LDA, and to estimate simultaneously the response of the sand bed by a photometric method. Estimates showed that displacement of the fluid-sand interface from the equilibrium position on the photopictures was measured within an accuracy of 0.5 mm.

The flow kinematic parameters were measured using a laser Doppler anemometer (LDA DANTEC). A LDA-system consisted of two beams having diameters 1 mm, one component modular optics operating in the direct-scatter mode. Small particles (1 - 5 μm), which are commonly present in most liquids, provided the necessary scattering centers. The kinematic data were recorded and processed using a data acquisition and signal processor system and a personal computer with special software. The velocity and arrival-time information were stored to reconstruct the mean velocity, RMS-value, and Turbulent Intensity (TI). For these experiments the signal processor was set for a Doppler frequency range of 0.12 MHz or 0.40 MHz. A frequency shift of 40 MHz was used for the Doppler frequency ranges. These settings for the red light (wavelength = 632.8 nm) covered the expected velocity range of -0.4 to 1.1 m/s, respectively. The vertical velocity profiles were obtained by displacing the modular optics by means of a

traverse mechanism. Measurements were made at various heights above the bed at horizontal positions equally spaced over one wavelength of the bottom undulation. The combined relative error of the velocity measurement did not usually exceed 3%. Most of the velocity measurements outlined in this paper were made at distance from 0.2 to 0.4 m from the leading edge of the undulated section of bed.

4. RESULTS AND DISCUSSION

4.1. Flow over a movable sediment bed

Experiments showed that for certain intervals of the Froude number, F , the surface of movable bed was characterized by periodic irregularities - sand waves.

If the flow is tranquil, $F < 1$, ripples and dunes could be generated. These sand waves are similar in shape: they have the upstream side with gradually varying slope and the abrupt downstream side. Introducing the length L and amplitude a of sand waves, and considering the characteristic scale of uniform flow to be the depth h , it is possible to distinguish ripples and dunes: in the case of ripples L and a are not functions of h , whereas for dunes they depend on h . These waves move in the direction of flow with velocity u_s (< 0.5 cm/s) which is small in comparison to the velocity U of uniform flow.

Figure 1 shows the theoretical curve derived from Eq. (1) and experimental data. These results can be used as the basis to estimate different bedforms: if the velocity U and the depth h are known, that wavelengths of dunes and antidunes can be predicted. The main discrepancy between the predicted and experimental values of F is due to following factors. First, experiments say that as a rule, bedforms had a random, unsteady and three-dimensional structure, whereas the model was deterministic and two-dimensional. Note that the case of 3D-bedforms was considered by Reynolds (1965). His modified criterion for the maximum Froude number was in better agreement with measured data but did not compensate for the discrepancy. Second, in the Kennedy-Reynolds' model the sediment transport was considered in the vicinity of the bed (so-called 'bed-load transport'), notwithstanding the transport of suspended material. Finally, the model was derived in the approximation of ideal fluid. All this is well-known and described in greater detail in many places.

To simplify the complicated problem of fluid flow over a sediment bed, an attempt was made to consider only the fluid region over a rigid undulated bottom.

4.2. Flow over undulated rigid bottom

Experiments have been performed to determine the near-bottom velocity field. These results are necessary to an understanding of the response of the bed to the uniform flow in the fluid area.

The original bed profile is shown in detail as the full line in the lower part of Fig. 2(a). The bed wavelength was $L = 11.4$ cm, so its steepness was $ak = 0.25$. The flow above the zero streamline $\psi = 0$ displays the expected features, namely that the streamlines converge over crests and diverge over the troughs. The consequence of this may be seen in Fig. 2(b), where measured and predicted (See Eq.(6)) vertical profiles of horizontal velocity u are shown. At the crest the surface velocity is $1.27U$, where U is the undisturbed free-stream velocity, and at the trough the surface velocity is $0.68U$. The velocity perturbation due to the bed form extends throughout the area of the flow up to free surface because water is relative shallow compared with the bed wavelength ($h/L=0.39$). The presence of a free surface caused relative increases in velocity over crests, and relative decreases in the troughs. The theory is in good agreement with the experimental data.

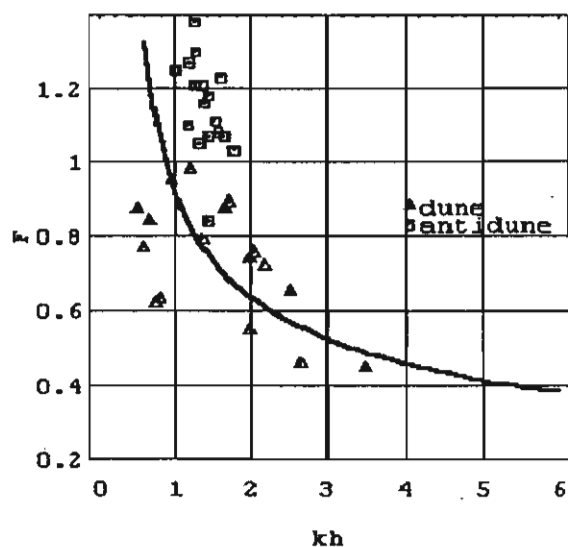


Figure 1. Comparison of predicted and observed forms

The dependence of results upon kh is expected on the basis of the results for perturbed potential flow. Fig. 3 shows the flow features in the case $kh = 3.85$.

Note that in near-bottom and near-free-surface regions, the measured velocity profiles deviate from the theoretical profiles. There are three major reasons for the deviations observed in the LDA measurements: 1) velocity information is integrated over the finite size of the measuring volume. For a zero or small velocity gradient, this integration does not affect the mean values. However, if the velocity gradient is changing, this effect becomes important; 2) LDA measurements are discrete and, therefore, the measurements at different points in a velocity profile must be phase-related. In this respect, in addition to errors relating to the phase trigger accuracy, the fluctuations in the driving frequency during the measurements must be added. These errors could not be accurately estimated;

3) in very-near-bottom or free surface regions, reflections from bed or free surfaces are collected by the receiving optics. These reflections contain the shift frequency and are detected as zero velocity. For larger velocities, the signal evaluation algorithm can reject such influences. For small velocities, this effect leads to lower velocity estimates. The effect could be reduced if refractive-index matched device was used (Teufel *et al.*, 1992).

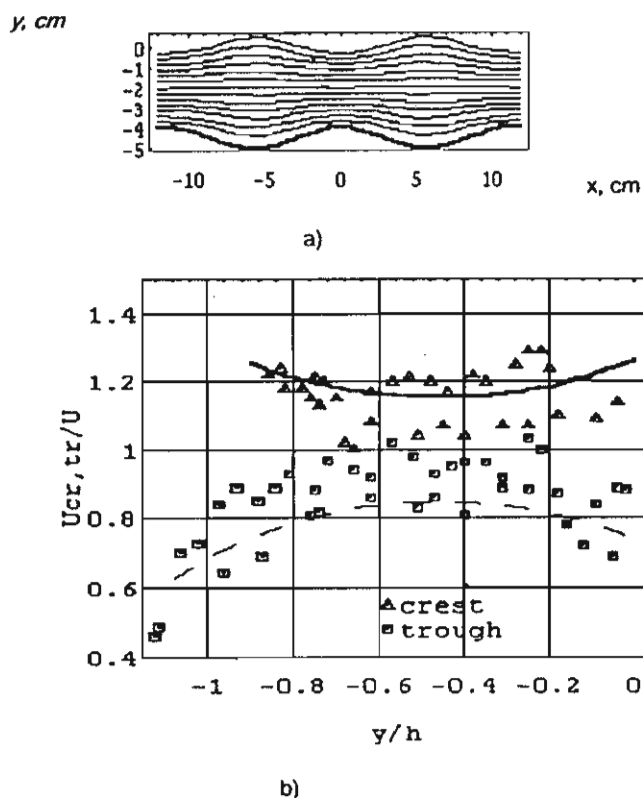


Fig. 2. a) Streamlines for nonseparating flow over the undulated rigid bottom; b) Vertical profiles of the normalized horizontal velocity above crest and trough positions: $U = 38$ cm/s, $a = 0.5$ cm, $L = 11.4$ cm

In Fig. 4 the mean velocity u/U and turbulent intensity (TI) at three different levels are plotted as functions of downstream distance. Dots represent model results. In spite of the scatter of experimental points, the model calculation exhibits the major features of the flow. In particular, note the profiles at $y = -5.8$ cm and $y = -5.0$ cm above bed. The calculation indicates that at these levels the flow decelerates initially and then accelerates farther downstream, and the data support this fact. A related result of spacial non-homogeneity was obtained by McLean and Smith (1986) in studies of the flow over a large sand waves (2.7 m high and 74 m long) in Columbia River.

The extreme values of horizontal flow velocity over crests and troughs as functions of bedform steepness, and the results of calculations (See Eq. (9)) are plotted in Fig. 5. The

dimensionless velocity increases at the crest and decreases at the trough as the steepness ak increases.

The measured values of u obeyed the linear curve in the semi-log plot. Therefore, the friction velocity u_* could be evaluated from the general log-law with the von Karman constant 2.5. The friction velocity may be used to determine the shear stresses τ_0 exerted on bottom undulations by a turbulent fluid stream. For bedforms, the basic parameters affecting the friction f are the water density and dynamic viscosity, the friction velocity u_* , the average flow depth h , the undulation amplitude a , and the bed length L .

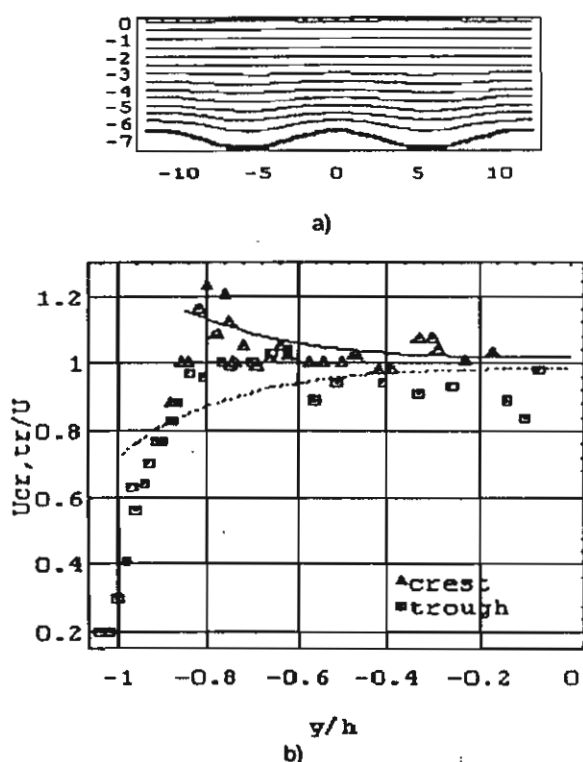


Figure 3. a) Streamlines for nonseparating flow over the undulated rigid bottom; b) Vertical profiles of the normalized horizontal velocity above crest and trough positions: $U = 24.5$ cm/s, $a = 0.7$ cm, $L = 11.4$ cm

The results in Figures 6 and 7 are for symmetrical triangular bedforms, and calculations have been performed by adopting the choice seven harmonics in Fourier series form. This is thought to give a good compromise between experimental and model profiles.

6. CONCLUSIONS

The flow pattern over an undulated rigid bottom has been considered, and the results of the experimental study are presented. The experimental observations have shown that the

bottom undulations have a significant effect upon both the mean velocity profiles and the magnitude of the turbulent fluctuations.

The overall agreement between the potential flow linear model and the measurements of the horizontal average of the time-mean velocity is surprisingly good in view of fact that this model was derived for non-separating flow. However, the horizontal velocity clearly deviates from calculated values in the immediate vicinity of the bed. This is probably due to the large-scale momentum exchanges associated with vortex formation.

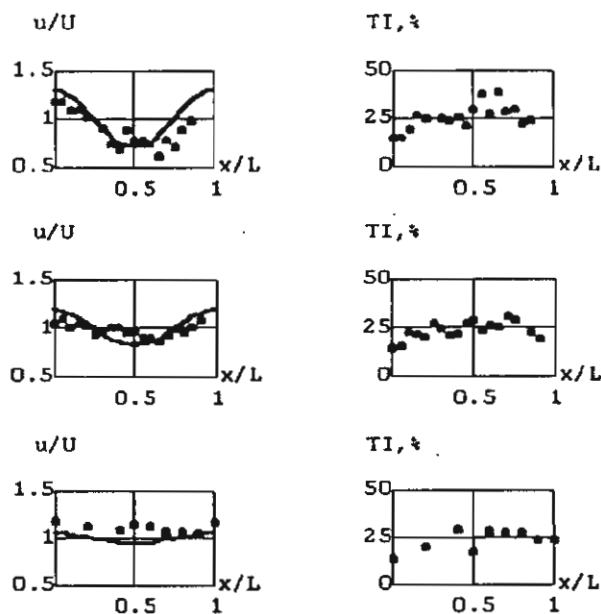


Figure 4. Horizontal distribution of mean velocity and turbulent intensity (TI) at level $y = -5.8$; -5.0 ; and -3.0 cm for flow velocity $U = 21$ cm/s and depth $h = 7.0$ cm, and bottom undulations with $L = 10.0$ cm and $a = 1.0$ cm

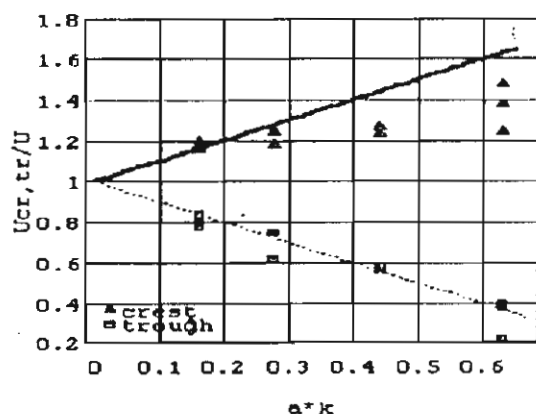


Figure 5. Dimensionless horizontal velocities u_{cr}/tr at crest and trough as functions of bedform steepness

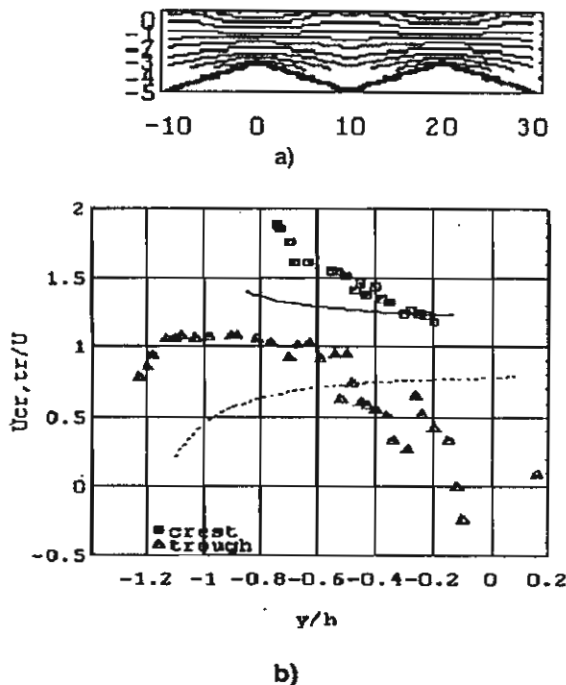


Figure 6. a) Streamlines for nonseparating flow over the "sawtooth" rigid bottom; b) Vertical profiles of the normalized horizontal velocity above crest and trough positions ($L = 20$ cm, $a = 1.0$ cm, $h = 4.0$ cm, $U = 33.5$ cm/s)

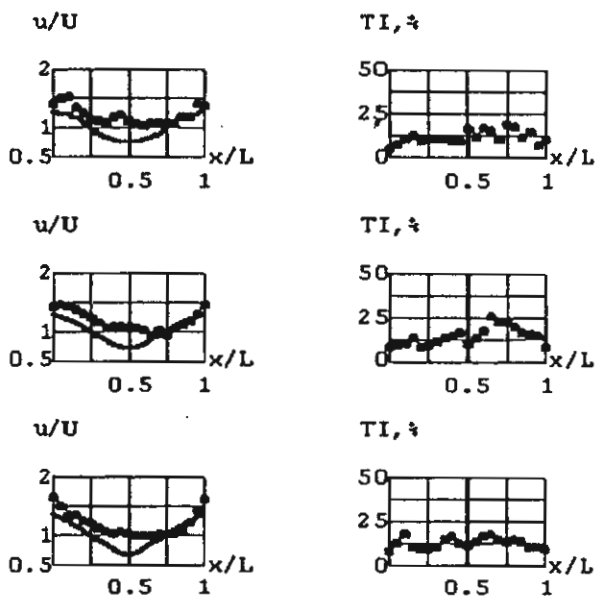


Figure 7. Horizontal distribution of mean velocity and turbulent intensity (TI) at level $y = -1.0$; -2.0 ; and -2.9 cm for flow velocity $U = 33.5$ cm/s and depth $h = 4.0$ cm, and bottom triangular undulations with $L = 20.0$ cm and $a = 1.0$ cm

ACKNOWLEDGMENTS

The research reported in this paper was supported in part by the Thai Research Fund (Grant No. RSA 3880019) and by the Russian Foundation for Fundamental Research (Project No. 96-01-00265).

REFERENCES

- Davies, A.G., 1979, "The potential flow over ripples on the seabed", *J. Marine Res.*, Vol. 39, pp. 743-759.
- Davies, A.G., 1983, "Wave interactions with rippled sand beds", in *Physical oceanography of coastal and shelf seas*, Johns B., ed., Elsevier, NY, pp. 1-65.
- Kennedy, J.F., 1963, "The mechanics of dunes and antidunes in erodible-bed channels", *J. Fluid Mech.*, Vol. 16, pp. 521-544.
- Kennedy, J.F., 1969, "The formation of sediment ripples, dunes and antidunes", *Ann. Rev. Fluid Mech.*, Vol. 1, pp. 147-168.
- Longuet-Higgins, M.S., 1981, "Oscillating flow over steep sand ripples", *J. Fluid Mech.*, Vol. 107, pp. 1-37.
- McLean, S.R., and Smith, J.D., 1986, "A model for flow over two-dimensional bed forms", *J. Hydraulic Eng.*, Vol. 112, pp. 300-317.
- Mel'nikova, O.N., 1996, "The formation of sand ridges by stationary waves at the bottom of a river flow", *Izvestiya, Atmospheric and Oceanic Physics*, Vol. 32, pp. 426-430.
- Mercer, A.G., and Haque, M.I., 1973, "Ripple profiles modeled mathematically", *ASME J. Hydraulic Div.*, Vol. 99, pp. 441-459.
- Ranasoma, K.I.M., and Sleath, F.A., 1994, "Combined oscillatory and steady flow over ripples", *ASME J. Waterw. Port Coastal Ocean Eng.*, Vol. 120, pp. 331-346.
- Reynolds, A.J., 1965, "Waves on the erodible bed of an open channel", *J. Fluid Mech.*, Vol. 22, pp. 113-133.
- Teufel, M., Trimis, D., Lohmüller, A., Takeda, Y., and Durst, F., 1992, "Determination of velocity profiles in oscillating pipe-flows by using laser doppler velocimetry and ultrasonic measuring devices", *Flow Meas. Instrum.*, Vol. 3, pp. 95-101.
- Van Rijn, L.S., Nieuwjaar, M.W.C., Kaay, T., Nap, E., and Kampen, A., 1993, "Transport of fine sands by currents and waves", *ASME J. Waterw. Port Coastal Ocean Eng.*, Vol. 119, pp. 123-143.

Wongwises, S., Effect of inclination angles and upper end conditions on the countercurrent flow limitation in straight circular pipes, *Int. Comm. Heat Mass Transfer*, 1998; 25(1):117-125.

January 1998

ISSN 0735-1933

UB/TIB Hannover



L tec Z 463

ZN 6500

1998 : 25,1

International Communications in
HEAT and MASS
TRANSFER

PERGAMON

INTERNATIONAL COMMUNICATIONS IN HEAT AND MASS TRANSFER

1998

Volume 25, Number 1

January

Contents

D. Yan and S.S. Cha	1	Practical common-path interferometry for real-time thermal/fluid flow measurements
Y. Li and C.-W. Park	9	Prediction of mass transfer rate in fibrous and granular media using packing permeability
S.F. Benjamin and C.A. Roberts	19	Warm up of automotive catalyst substrates: Comparison of measurements with predictions
G. Polidori, M. Lachi and J. Padet	33	Unsteady convective heat transfer on a semi-infinite flat surface impulsively heated
T. Aicher and W.K. Kim	43	Experimental investigation of the influence of the cross flow in the nozzle region on the shell-side heat transfer in double-pipe heat exchangers
P. Venkateswarlu and P. Gopalakrishna	59	A simplified method for correlating mass transfer data in electrochemical cells
C.W. Leung and H.J. Kang	67	Convective heat transfer from simulated air-cooled printed-circuit board assembly on horizontal or vertical orientation
R. Kumar, H.K. Varma, B. Mohanty and K.N. Agrawal	81	Augmentation of outside tube heat transfer coefficient during condensation of steam over horizontal copper tubes
D.C. Erickson, A. Gomezplata and R.A. Papar	93	Use of the Colburn-Drew equations to model mass transfer
H.A. Abdel-Aal	99	Error bounds of variable conductivity temperature estimates in frictionally heated contacts
J. Drchalová and R. Černý	109	Non-steady-state methods for determining the moisture diffusivity of porous materials
S. Wongwises	117	Effect of inclination angles and upper end conditions on the countercurrent flow limitation in straight circular pipes
S. Theerakulpisut and S. Priprem	127	Modeling cooling coils
D.A. Tarzia	139	The determination of unknown thermal coefficients through phase change process with temperature-dependent thermal conductivity
	149	Announcement

INDEXED IN Current Contents, Eng. Ind. Monthly and Author Ind., Energy Res. Abstr., EDB, and the MSCI



Pergamon



ISSN 0735-1933

IHMTDL 25 (1) 1-150 (1998)
(208)



0735-1933(199801)25:1;1-M



Pergamon

Int. Comm. Heat Mass Transfer, Vol. 25, No. 1, pp. 117-125, 1998
Copyright © 1998 Elsevier Science Ltd
Printed in the USA. All rights reserved
0735-1933/98 \$19.00 + .00

PII S0735-1933(97)00143-7

EFFECT OF INCLINATION ANGLES AND UPPER END CONDITIONS ON THE COUNTERCURRENT FLOW LIMITATION IN STRAIGHT CIRCULAR PIPES

Somchai Wongwises
Department of Mechanical Engineering,
King Mongkut's Institute of Technology Thonburi, Thailand
Bangmod, Bangkok 10140, Thailand

(Communicated by J.P. Hartnett and W.J. Minkowycz)

ABSTRACT

In the present study, the experimental data of the countercurrent flow limitation (CCFL) for air and water in inclined pipes are investigated. Water is introduced at the top of the test section while air is injected at the bottom as countercurrent flow. The water flow rate is fixed while the air flow rate is slowly increased, until the CCFL is reached. Data from each experiment consists of the flow rates of air and water. The curves of CCFL are built and shown as a function of the dimensionless superficial velocity. The influence of the inclination angles of the pipes and upper end conditions on CCFL are also discussed.

© 1998 Elsevier Science Ltd

Introduction

Countercurrent flow limitation (CCFL) or the onset of flooding refers to the limiting condition at which the flow rates of both the gas and the liquid phase cannot be increased further. A further increase will cause the liquid to be carried by the gas. This is a subject of engineering interest, particularly in the design of two-phase heat and mass transfer processes.

Many studies have been carried out, both experimentally and analytically on CCFL, mostly in vertical pipes [1,2,3,4]. The CCFL in an inclined pipe has received comparatively very little attention in the literature. Some of the earliest work was performed by Barnea et. al. [5] with particular attention on the effect of the water inlet sections. Two types of water inlet sections, an inner tube section and a porous section, are used in the experiments. Data on flooding were collected and predictive models for calculating the flooding conditions were proposed.

Celata et. al. [6,7] evaluated the influence of slight deviations from the vertical position on the flooding parameters in a circular pipe, with and without obstructions respectively. An improvement on the

Barnea et. al. model for the prediction of the onset of flooding in inclined pipes was proposed. Geweke et.al. [8] investigated the influence of pipe diameter and the inclination angle on the flooding limit. Angles of 5° to 50° from the horizontal were chosen. A new calculation procedure based upon a two-fluid model was developed.

Relatively little information is currently available on the countercurrent flow limitation or flooding phenomena in inclined circular pipes. The effect of the inclination angles and the upper end conditions have not yet been clearly investigated. In the present study, the experimental results of the CCFL of air and water in inclined circular pipes are obtained and the effects of a small inclination angle from the vertical and upper end condition of the test section are investigated.

Experimental Apparatus and Method

A schematic diagram of the test facility is shown in Fig 1. In the experimental investigations, air and water were used as the working fluids. The main components of the system consisted of the test section, an air supply, a water supply and instrumentation. The test section, with an inside diameter of 29 mm the length of 3.50 m was constructed from transparent acrylic glass to permit visual observation of the flow patterns. The connections of the piping system were designed such that the component part can be changed very easily. Water was pumped from the storage tank through a rotameter, to the water inlet section and hence flowed back to the storage tank. The water inlet section (Fig. 2) was constructed from two concentric tubes, the inner tube being the test section or sinter which was radially drilled with 350 holes of 1 mm diameter. The inner tube of the sinter was also covered with a fine wire mesh to distribute the water smoothly along the inclined pipe.

The water in the inlet section flowed downwards to the storage tank while the air flowed countercurrently. The level of water in the water outlet section was kept constant, and the excess water was returned to the storage tank. Two types of upper end conditions (open and closed) (see Fig.1) were used in the experiments. Air was supplied to the test section by a blower and the air flow was controlled by a valve at the outlet of a blower. The inlet flow rate of air was measured by means of an orifice and micromanometer, and the inlet flow rate of water was measured by three sets of rotameter within the range of $0\text{--}4.8\text{ m}^3/\text{h}$. The temperatures of air and water were measured by thermocouples ($\pm 0.5\%$). The two phase pressure drop between the test section was measured by a digital manometer within resolution of 0.1 Pa.

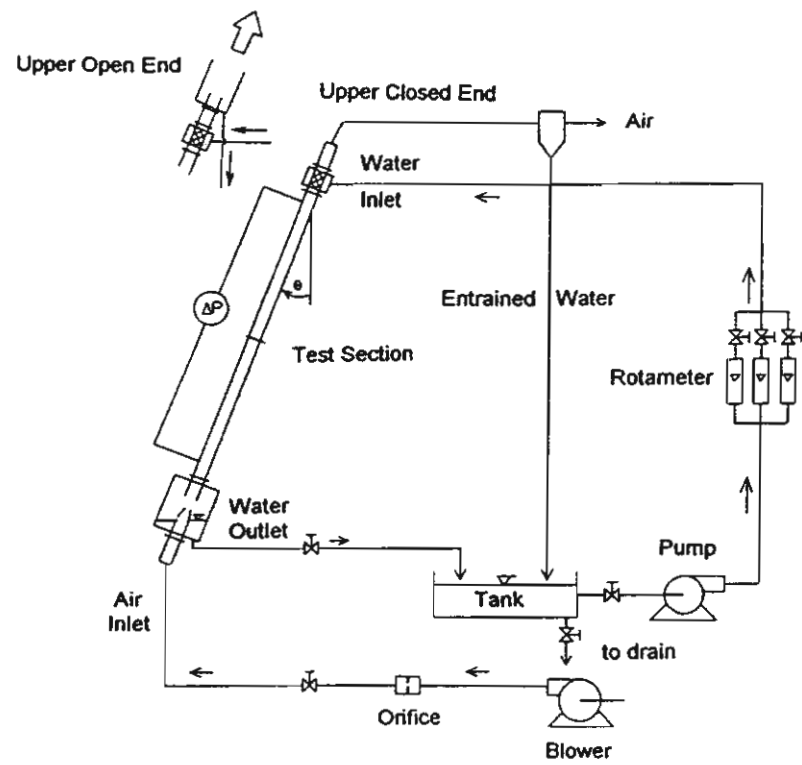


FIG. 1
Schematic diagram of experimental apparatus

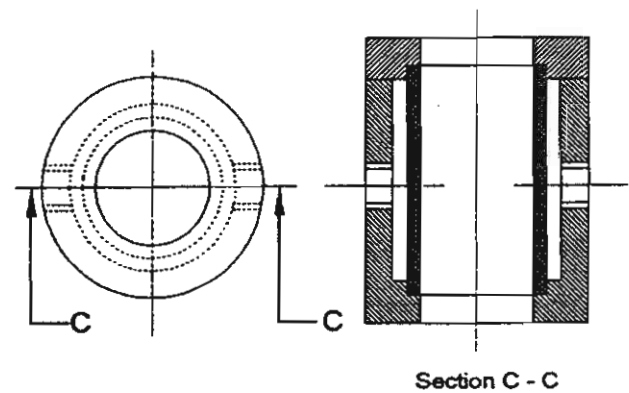


FIG. 2
Schematic diagram of water inlet section

Experiments were conducted at various air and water flow rates, at varying inclination angles from the vertical (θ) and a variety of upper end conditions. In the experiments the air flow rate was increased by small increments while the water flow rate was kept constant at a preselected value. After each change in the inlet air flow rate, both the air and water flow rates were recorded. The experiments were continued until the onset of flooding was observed.

Results and Discussion

The countercurrent flow limitation was determined by keeping the injected water flow rates constant, while the air flow rate was increased in small increments up to the onset of flooding. Flooding was observed visually in conjunction with the pressure drop. For small air flow rates, the water flows downward from the water inlet section through the test section to the storage tank. In this case the superficial velocities of the water phase at the water inlet and water outlet section were equal. As the air flow rate was gradually increased, the pressure drop of two-phase flow increased slightly. At the onset of flooding, due to instabilities at the interface, slugging occurred and the pressure drop suddenly increased. The slugs carry a fraction of the injected water to the upper end section: the water flow at the water outlet section is thus smaller, and afterwards the pressure drop decreased.

Typical flooding curves connecting all points of the onset of flooding are shown in Figs 3 to 8. They show the relationship between the square root of the dimensionless superficial velocity of water $(j_L^*)^{1/2}$ with the square root of the dimensionless superficial velocity of air $(j_G^*)^{1/2}$. The variables j_L^* , j_G^* are defined by

$$j_k^* = j_k \left[\frac{\rho_k}{(\rho_L - \rho_G)gD} \right]^{1/2}, \quad k = G, L$$

where j_k and ρ_k denote the superficial velocity and density, respectively, of phase k ; g is the gravitational acceleration; and D is the pipe diameter.

At specific experimental conditions the onset of flooding was found to depend on the inlet feed water flow rate. The air flow rate creating the onset of flooding decreased as the water flow rate increased. The effect of the inclination angle from the vertical is shown in Figs. 3 and 4. In the case of an upper open end, the water flows along nearly vertical inclined pipes were accelerated by gravity and tended to depress the growth of unstable waves. A greater air flow rate was therefore required to cause flooding. The effect

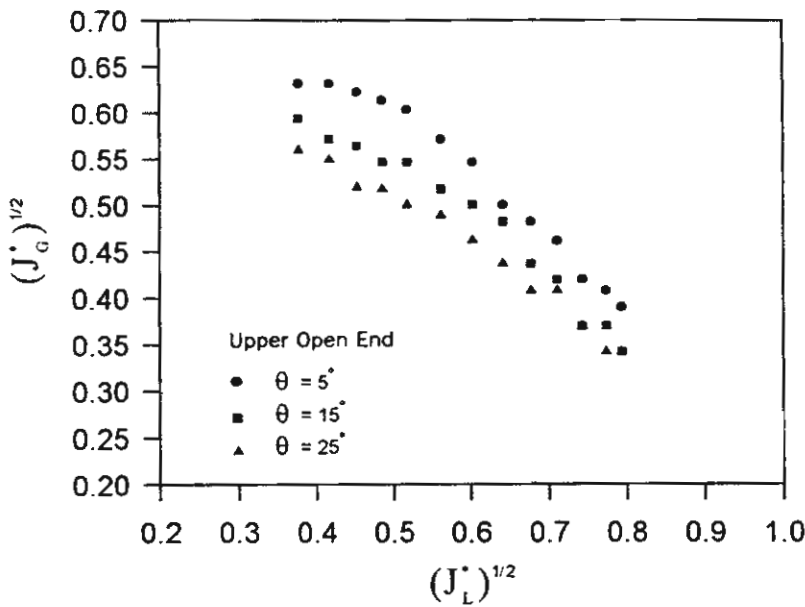


FIG. 3

Effect of inclination angle from the vertical (θ) on flooding

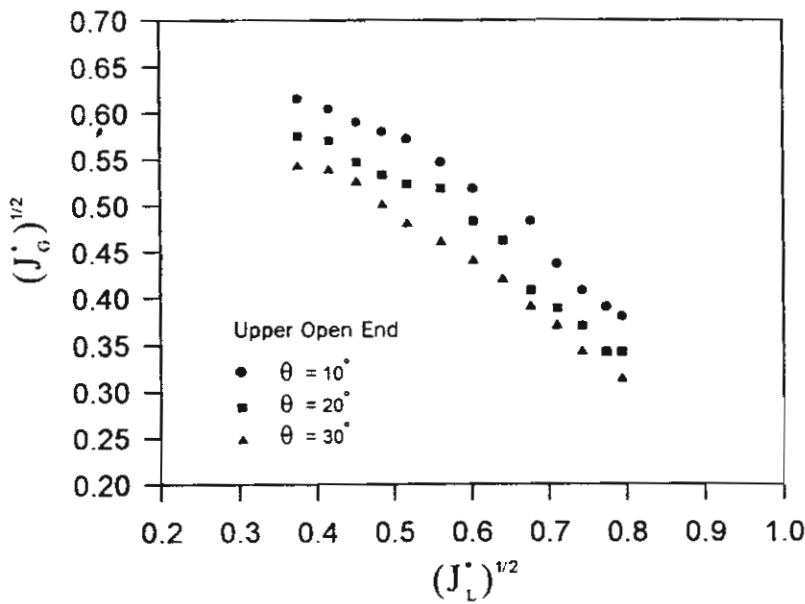


FIG. 4

Effect of inclination angle from the vertical (θ) on flooding

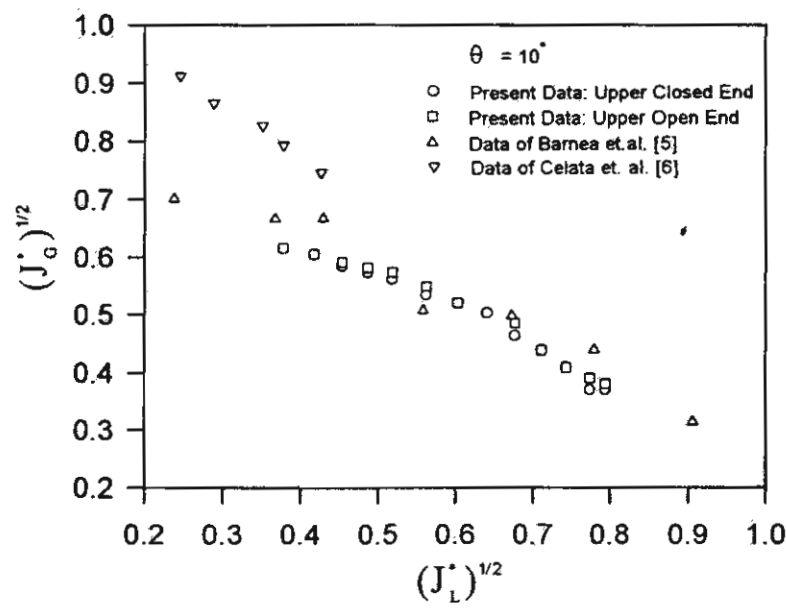


FIG. 5

Effect of upper end condition on flooding for the inclination angle from the vertical $(\theta) = 10^\circ$

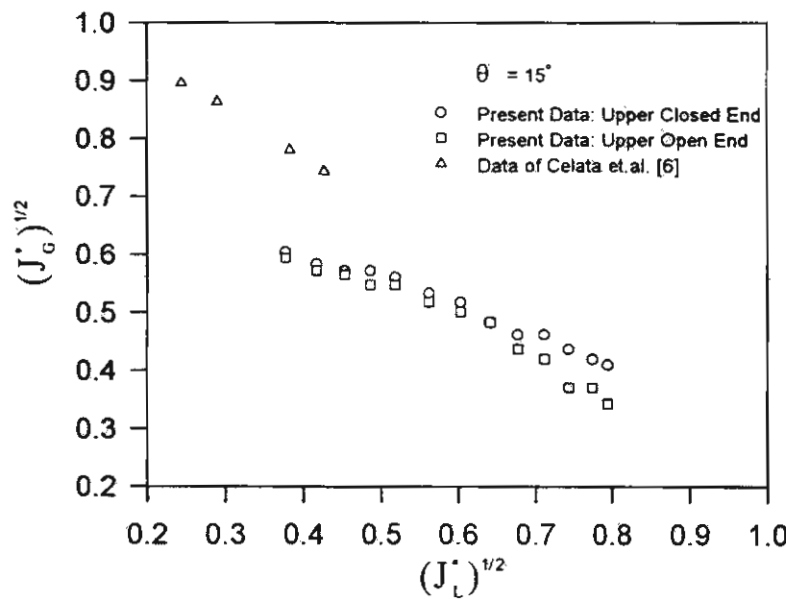


FIG. 6

Effect of upper end condition on flooding for the inclination angle from the vertical $(\theta) = 15^\circ$

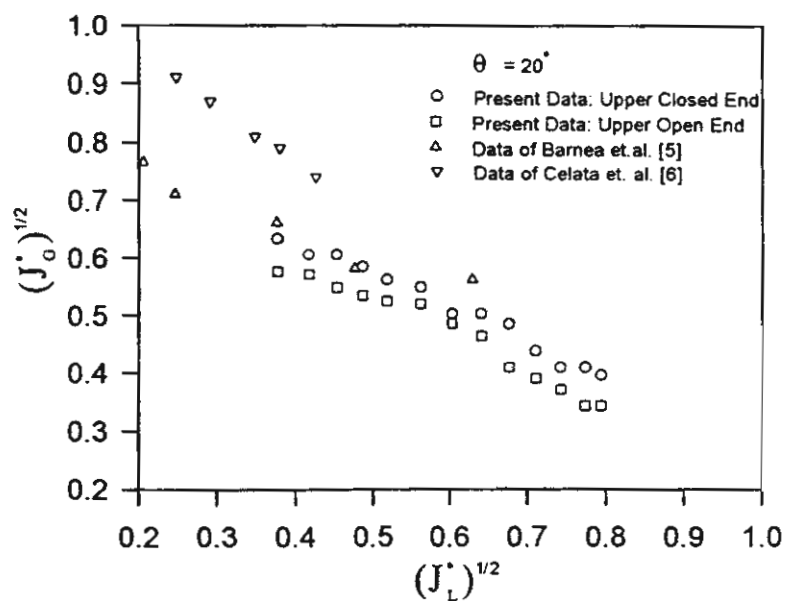


FIG. 7

Effect of upper end condition on flooding for the inclination angle from the vertical (θ) = 20°

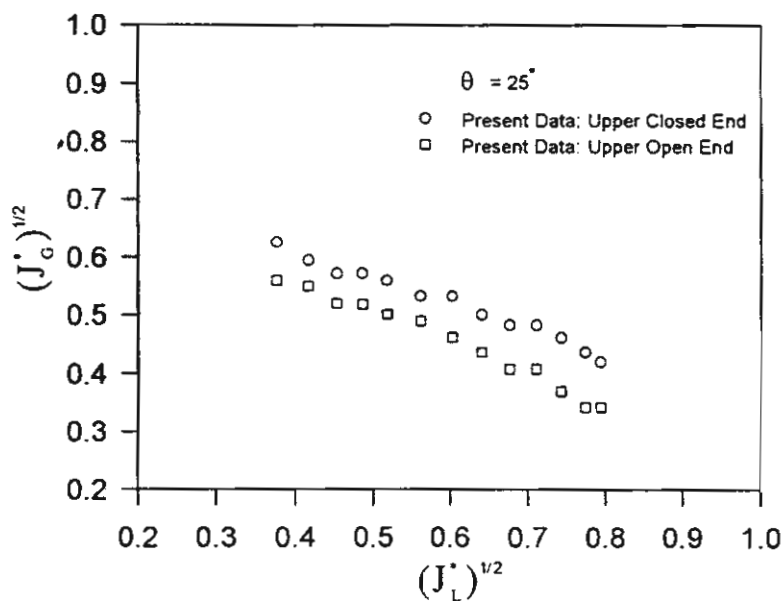


FIG. 8

Effect of upper end condition on flooding for the inclination angle from the vertical (θ) = 25°

of inclination angles is closely related to the condition of the upper end. For an upper closed end condition, the onset of flooding is nearly the same for all inclination angles from the vertical position. This means that the flooding points of the open system and the closed system become more distinct as the inclination angle from the vertical was increased. (Figs. 5 to 8). The results are also compared with those from Barnea et.al. [5], $D = 51$ mm and Celata et.al. [6,7], $D = 20$ mm and shown in Figs. 5 to 7. The data points from Barnea et.al. [5] are taken from a log-log plot, thus causing some uncertainties. Therefore only some points are shown in the figures. However the results from Barnea et.al. correlated quite well with those of this study in the case of an upper closed end system.

Conclusion

This paper presents new data for countercurrent flow of gas and liquid in a pipe which is slightly inclined from the vertical. Experiments were performed to determine the countercurrent flow limitation (or onset of flooding). Water was ejected through the test section while air flowed countercurrently and the phenomena was visually observed. The general flooding points depend on the water feed rate. The air flow rate which causes the onset of flooding decreases while the water flow rate increases. The influence of the inclination angle and upper end conditions is of significance for the onset of flooding. For an upper-open end system, with increasing inclination angles from the vertical, the flooding curves shift to lower gas velocities. For an upper-closed end system, the onset of flooding is nearly the same for all inclination angles. The difference of flooding points between two types of upper end conditions become large when the inclination angle is increased.

Acknowledgments

The present study was supported financially by the Thailand Research Fund (TRF) whose guidance and assistance are gratefully acknowledged. The author also express gratitude to Mr. Amnaj Koomanee, Mr. Opas Klaengnuan, Mr. Weerachai Kanchanamai, Mr. Thammasak Saengnoi and Mr. Pitiporn Hasuankwan from the Department of Mechanical Engineering, King Mongkut's Institute of Technology Thonburi for their assistance in some of experimental work.

Nomenclature

D	pipe diameter, m
g	gravitational acceleration, m/s^2
j	superficial velocity, m/s
j^*	dimensionless superficial velocity

Greek Symbols

- θ inclination angle from the vertical, deg.
 ρ density, kg/m³
 ΔP pressure drop, Pa

Subscripts

- k gas or liquid
G gas
L liquid

References

1. C.L. Tien and C.P. Liu, Survey on Vertical Two-Phase Countercurrent Flooding. EPRI Rep. NP-984, (1979).
2. S.G. Bankoff and S.C. Lee, A Comparison of Flooding Models for Air-Water and Steam-Water Flow, *Proc. Advances in Two-Phase Flow and Heat Transfer*, vol. 2, pp.745-780, S. Kakac and M. Ishii, Eds., NATO ASI Series (1983).
3. W.A. Ragland and E.N. Ganic, Flooding in Countercurrent Two-Phase Flow, *Proc. Advances in Two-Phase Flow and Heat Transfer*, vol. 2, pp.505-538, S. Kakac and M. Ishii, Eds., NATO ASI Series (1983).
4. Y. Koizumi and T. Ueda, *Int.J. Multiphase Flow* 22, 31 (1996).
5. D. Barnea, N. Ben Yoseph and Y. Taitel, *Can. J. Chem. Eng.* 64, 177 (1986).
6. G.P. Celata, M. Cumo and T. Setaro, Flooding in Inclined Pipes, *Proc. Advances in Gas-Liquid Flow*, FED-Vol.99, HTF-Vol.155, pp. 229-235, J.H.Kim, U.S. Rohtagi, and A. Hashemi, Eds., ASME (1990).
7. G.P. Celata, M. Cumo, G.E. Farello and T. Setaro, *Exp. Thermal & Fluid Sci.* 5,18 (1992).
8. M. Geweke, H. Beckmann and D. Mewes, *European Two-Phase Flow Group Meeting*, Stockholm, Paper J1, (1992).

Received August 25, 1997

Wongwises, S., Interfacial Friction Factors in Countercurrent Stratified Two-Phase Flow in a Nearly-Horizontal Circular Pipe, *Int. Comm. Heat Mass Transfer*, 1998; 25(3): 369-377.